UC Davis

UC Davis Previously Published Works

Title

Differential response of pineal microglia to surgical versus pharmacological stimuli

Permalink

https://escholarship.org/uc/item/4kf0h0x0

Journal

The Journal of Comparative Neurology, 526(15)

ISSN

1550-7149

Authors

Rodriguez, María P Ibañez
Galiana, María D
Rásmussen, Jorge A
et al.

Publication Date

2018-10-15

DOI

10.1002/cne.24505

Peer reviewed

eScholarship.org Powered by the California Digital Library
University of California

Author Manuscript

Author Manuscript

Author Manuscript

Author Manuscript

HHS Public Access

Author manuscript

J Comp Neurol. Author manuscript; available in PMC 2019 October 15.

Published in final edited form as:

J Comp Neurol. 2018 October 15; 526(15): 2462–2481. doi:10.1002/cne.24505.

Differential Response of Pineal Microglia to Surgical versus Pharmacological Stimuli

María P. Ibañez Rodriguez[1], **María D. Galiana**[1], **Jorge A. Rásmussen**[1], **Carlos L. Freites**[1], **Stephen C. Noctor**[2], and **Estela M. Muñoz**[1]

[1]Institute of Histology and Embryology of Mendoza (IHEM), National University of Cuyo, National Scientific and Technical Research Council (CONICET), Mendoza, Argentina.

[2]Department of Psychiatry and Behavioral Sciences, MIND Institute, University of California, Davis, School of Medicine, Sacramento, CA, United States of America.

Abstract

Microglial cells are one of the interstitial elements of the pineal gland (PG). We recently reported the pattern of microglia colonization and activation, and microglia-Pax6$^+$ cell interactions during normal pineal ontogeny. Here, we describe the dynamics of microglia- Pax6$^+$ cell associations and interactions after surgical or pharmacological manipulation. In adult rats, the superior cervical ganglia (SCG) were exposed, and either bilaterally excised (SCGx) or decentralized (SCGd). In the SCGx PGs, the density of Iba1$^+$ microglia increased after surgery and returned to sham baseline levels 13 days later. Pineal microglia also responded to SCGd, a more subtle denervation. The number of clustered Iba1$^+$/PCNA$^+$/ED1$^+$ microglia was higher four days after both surgeries compared to the sham-operated group. However, the number of Pax6$^+$/PCNA$^-$ cells and the percentage of Pax6$^+$ cells contacted by and/or phagocytosed by microglia increased significantly only after SCGx. Separate groups of rats were treated with either bacterial lipopolysaccharides (LPS) or doxycycline (DOX) to activate or inhibit pineal microglia, respectively. Peripheral LPS administration caused an increase in the number of clustered Iba1$^+$/PCNA$^+$/ED1$^+$ microglial cells, and in the percentage of Pax6$^+$ cells associated with and/or engulfed by microglia. In the LPS-treated PGs, we also noted an increase in the number of PCNA$^+$ cells that were Iba1$^-$ within the microglial cell clusters. The density of Pax6$^+$ cells did not change after LPS treatment. DOX administration did not influence the parameters analyzed. These data suggest that pineal microglia are highly receptive cells capable of rapidly responding in a differential manner to surgical and pharmacological stimuli.

Address reprint requests to Estela M. Muñoz, IHEM, UNCuyo, CONICET, CC: 56, Av. Libertadores 80, Parque General San Martín, Mendoza, CP: 5500, Argentina. munoz.estela@fcm.uncu.edu.ar or cj26me@yahoo.com.

AUTHOR CONTRIBUTIONS

MPIR, SCN and EMM designed the experiments. MDG, JAR and MPIR implemented the surgical procedures. MPIR performed the experiments, and collected and analyzed the data. SCN and EMM provided the resources. MPIR, JAR, CLF, SCN and EMM contributed to the original draft. MPIR, CLF, SCN and EMM wrote, reviewed, and edited the final version of the manuscript.

Pineal Iba1+/PCNA+/ED1+ microglia are constantly ‘activated’ cells able to sense and differentially respond to surgical and pharmacological stimuli. Here, we show how bilateral superior cervical ganglionectomy (SCGx) and decentralization (SCGd), and peripheral administration of bacterial lipopolysaccharides (LPS) and doxycycline (DOX) impact in a stimulus-specific manner on microglia, Pax6+ cells, and associations and interactions between both cell types within the pineal gland. We propose the pineal gland as an attractive model to study phagocyte renewal and the interface between the immune system and the central nervous system.

Author Manuscript Author Manuscript Author Manuscript Author Manuscript

Graphical Abstract

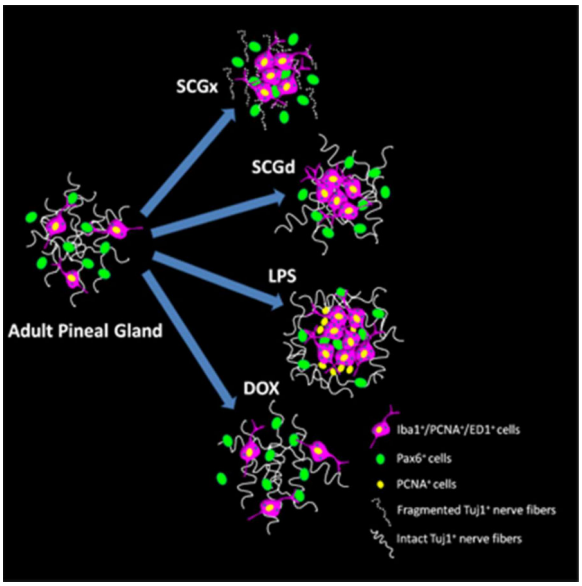

Keywords

microglia; pineal gland; differential responses; Iba1 (RRID: AB_2224402; RRID: AB_839504); Pax6 (RRID: AB_1566562; RRID: AB_2565003; RRID: AB_291612); ganglionectomy; decentralization; bacterial lipopolysaccharides; ED1 (RRID: AB_566872); Tuj1 (RRID: AB_10063408; RRID: AB_2313773); PCNA (RRID: AB_95106)

INTRODUCTION

Microglia are the primary innate immune cells in the central nervous system (CNS). These phagocytic cells constantly survey their local environment and play a role in the formation and homeostasis of the developing and adult brain, and protect the neural parenchyma from invading agents or injuries (Kettenmann, Hanisch, Noda, & Verkhratsky, 2011; Raivich, 2005; Reemst, Noctor, Lucassen, & Hol, 2016; Soulet & Rivest, 2008; Wake, Moorhouse, Miyamoto, & Nabekura, 2013). Microglial cells are highly dynamic in shape and function. Studies of the macrophage-specific plasma membrane glycoprotein F4/80, for example, revealed high plasticity in morphology and density of the microglia depending on their location in the healthy adult mouse brain (Gordon, Pluddemann, & Martinez Estrada, 2014; Lawson, Perry, Dri, & Gordon, 1990). This suggests that variations in the microglial cell microenvironment caused by proximity to neuronal and glial cell types, diversity of locallyreleased neurotransmitters, chemokines and cytokines, status of the local blood-brain barrier (BBB), among other factors, can affect microglia phenotype. Grabert et al. (Grabert et al., 2016) performed the first genome-wide analysis of mouse microglia and showed brain region-specific diversity in microglial transcriptional identity, sensitivity to dysregulation and involvement in age-related neurodegeneration.

Author Manuscript Author Manuscript Author Manuscript Author Manuscript

Recent work has demonstrated that 'resting' microglia in the healthy CNS are not passive macrophages that can be driven into an activated state by pathogens or damage, but instead are highly active cells (Kettenmann et al., 2011; Raivich, 2005). Microglia activation is a complex and multistage process that depends not only on the nature, but also on the intensity and persistence of the stimulus (Walker, Nilsson, & Jones, 2013). 'Activated' microglial cells can migrate to the site of injury and proliferate, and are associated with phagocytosis of cells and cellular components.

Like other macrophages, activated microglia were initially classified based on their functional polarization into two subtypes: 'classically activated' M1 pro-inflammatory or 'alternatively activated' M2 anti-inflammatory cells (Kigerl et al., 2009). However, this classification scheme does not fully encompass the range of functional phenotypes. Recent definitions consider the M1 and M2 subsets as extremes along a continuum of macrophage activation states (Martínez & Gordon, 2014; Ransohoff, 2016; Sica & Mantovani, 2012), with the balance between pro-inflammatory and anti-inflammatory signals determining microglial cell phenotype and responsiveness (Ajmone-Cat, Mancini, De Simone, Cilli, & Minghetti, 2013; Ajmone-Cat, Nicolini, & Minghetti, 2003; Cacci, Ajmone-Cat, Anelli, Biagioni, & Minghetti, 2008; Ekdahl, Kokaia, & Lindvall, 2009; Li, Lu, Tay, Moochhala, & He, 2007; Wolf, Boddeke, & Kettenmann, 2017).

Microenvironment-induced transitions between the resting and activated states reflect the plasticity of microglial cells within the CNS. However, in sites that lack a BBB, microglia display a constantly activated profile (Gordon et al., 2014; Lawson et al., 1990). We recently described the pattern of microglia colonization and activation during the ontogeny of a particular circumventricular organ (CVO), the pineal gland (PG). We proposed that microglial cells modulate pineal organogenesis and homeostasis by regulating the $Pax6^+$ cell population, especially in the adult gland, and also by remodeling signaling elements such as pinealocyte neurites, nerve fibers, and blood vessels (Ibanez Rodriguez, Noctor, & Muñoz, 2016). The $Pax6^+$ cells are thought to give rise to both pinealocytes and a subpopulation of glial cells during pineal ontogeny. In the mature PG, the $Pax6^+$ cells may represent a quiescent cell reservoir and a preferred target for the microglial cells (Ibanez Rodriguez et al., 2016; Rath, Rohde, Klein, & Moller, 2013). The study performed by Ibanez Rodriguez et al. (Ibanez Rodriguez et al., 2016) expanded the repertoire of microglial functions reported previously in the PG, including presentation of antigens, sensing and response to physical injury, bacteria and hypoxia, and regulation of melatonin production (da Silveira Cruz- Machado, Pinato, Tamura, Carvalho-Sousa, & Markus, 2012; Moller, Rath, & Klein, 2006; Pedersen, Fox, Castro, & McNulty, 1993; Pedersen et al., 1997).

The aim of this study was to analyze the plasticity and dynamics of the adult pineal microglia and their associations with $Pax6^+$ cells in adverse environments after surgical and pharmacological manipulations. The rhythmic pineal physiology is driven by the sympathetic innervation from the superior cervical ganglia (SCG) via post-ganglionic axons (Moller & Baeres, 2002). In adult rats, we disrupted the sympathetic innervation of the PG by either performing a bilateral surgical removal of the SCG (SCGx), or by performing a decentralization procedure of the SCG (SCGd), which severed the connection between the ganglion and the sympathetic nerve trunk but left the SCG and its efferent nerves intact

Author Manuscript Author Manuscript Author Manuscript Author Manuscript

(Hartley et al., 2015; Savastano et al., 2010). We also challenged separate groups of adult rats pharmacologically, either via intraperitoneal (IP) administration of gram-negative bacteria wall components, lipopolysaccharides (LPS) (Ajmone-Cat et al., 2003; Cacci et al., 2008; Cunningham, Martínez-Cerdeno, & Noctor, 2013; Jiang-Shieh et al., 2005; Li et al., 2007; Xie et al., 2017), or by IP administration of the antibiotic doxycycline (DOX), which is an inhibitor of microglial function (Jantzie, Cheung, & Todd, 2005; Lazzarini et al., 2013; Santa-Cecilia et al., 2016; Sultan, Gebara, & Toni, 2013; Yrjanheikki, Keinanen, Pellikka, Hokfelt, & Koistinaho, 1998). The manipulations applied here stem from our current understanding about the tight interplay between microglia and neuronal activity, and between microglia and inflammatory elements induced by peripheral insults, such as bacterial infections (Catorce & Gevorkian, 2016; Colonna & Butovsky, 2017; Wake et al., 2013; Xie et al., 2017).

Our data suggest that the constantly ‘activated’ microglia in the adult pineal gland represent a highly responsive and plastic cell population that reacts differentially to surgical and non-surgical insults.

MATERIALS AND METHODS

Animals

All animal procedures performed in this study followed the National Institutes of Health’s Guide for Care and Use of Laboratory Animals, the Animal Research: Reporting *in Vivo* Experiments (ARRIVE) Guidelines, and with approval by the Institutional Animal Care and Use Committee at the School of Medicine, National University of Cuyo, Mendoza, Argentina (Protocol IDs 9/2012 and 74/2016). All efforts were made to minimize the number of animals used and their suffering. Three-month-old male Wistar rats were maintained in temperature and humidity-controlled rooms under a 12:12 light:dark (L:D) cycle and with *ad libitum* access to food and water. Rats were euthanized by decapitation after ketamine/xylazine (50 and 5 mg/kg of body weight, respectively) anesthesia (Savastano et al., 2010), and pineal glands (PG) were collected during the light phase at *Zeitgeber* time (ZT) 6 and immediately processed for immunohistochemistry (IHC).

Surgical removal and decentralization of superior cervical ganglia

The superior cervical ganglionectomy (SCGx) was performed in adult rats as described in detail by Savastano et al. (Savastano et al., 2010). Decentralization of superior cervical ganglia (SCGd), on the other hand, involved removal of 2 to 3 mm of the sympathetic trunks immediately below the superior cervical ganglia (SCG), while keeping the ganglia and their efferent nerves to the pineal gland intact (Hartley et al., 2015; Savastano et al., 2010). Control animals underwent sham surgeries that included all steps along with the exposure of both SCG, but without their removal or decentralization. To define the kinetics of microglial cell number, SCGx and sham-operated animals were sacrificed at 3, 6, 9 and 13 days after surgeries (N=3 per group and per time point). To compare the effects of SCGd and SCGx on the number of $Iba1^+$ microglial cells, $Pax6^+$ cells, and microglia-$Pax6^+$ cell interactions, SCGx, SCGd and control animals were sacrificed 4 days after surgeries (N=4 per group).

Author Manuscript Author Manuscript Author Manuscript Author Manuscript

In vivo administration of doxycycline and bacterial lipopolysaccharides

The drugs were dissolved in sterile phosphate-buffered saline (PBS) and daily doses with a final volume not higher than 300 µl were injected intraperitoneally (IP) to adult rats at ZT6. The antibiotic doxycycline (DOX, D9891, Sigma-Aldrich, St Louis, MO, USA) was administered at 45 mg/kg of body weight for 7 days (Wang, Yang, Noor, & Shuaib, 2002; Yrjanheikki et al., 1998). The bacterial lipopolysaccharides (LPS, L4391, Sigma-Aldrich) were injected once per day on two sequential days at a concentration of 100 µg/kg of body weight (Cunningham et al., 2013). Control animals were treated with sterile PBS for 7 days. Five animals per group were used (N=5). The animals were sacrificed twenty-four (24) hours after the last injection.

Immunohistochemistry

Isolated pineal glands were fixed for immunostaining by immersion in 4% paraformaldehyde (PFA) in PBS at 4°C and subsequently processed as previously described (Ibanez Rodriguez et al., 2016). Briefly, the pineal glands were first embedded in Histoplast (Biopack, Bs. As., Argentina), and then ten-micrometer sections were cut at random orientations from the central area of each pineal gland using a Microm HM 325 microtome (Thermo Fisher Scientific Inc., Waltham, MA, USA). Slide-mounted tissues were hydrated and subjected to antigen retrieval by boiling in 0.01 M sodium citrate buffer (pH 6) containing (v/v) 0.05% Tween-20 for thirty minutes. Non-specific labeling was blocked by using (v/v) 10% donkey serum, 1% Triton X-100 and (w/v) 0.2% gelatin in PBS, for 1 hour at room temperature (RT) in a humid chamber. Immunolabeling was performed using primary antibody buffer containing specific antibodies (Table 1), (v/v) 2% donkey serum, 1% Triton X-100, and (w/v) 0.2% gelatin in PBS, overnight at RT. Sections were rinsed in PBS and then incubated in the secondary antibody buffer for 2 hours at RT. Secondary antibodies with low cross-reactivity, generated in donkey and conjugated with Alexa Fluor 488, Cy3 and Alexa Fluor 647, were used in a dilution 1:200 (Table 2). Slices were rinsed and covered with Mowiol mounting medium [(w/v) 9.6% Mowiol 4–88 (81381, Sigma-Aldrich) and 24% glycerol in 0.1M Tris- HCl buffer (pH 8.5)]. Primary antibodies were routinely omitted to determine non-specific labeling. The optimal antiserum concentrations were defined by initially immunostaining pineal gland sections with each primary antibody alone, using the dilution series recommended by the manufacturers. Double staining with the cocktails of primary antibodies was then performed, and the results were compared to those obtained from single antibody immunostaining. Imaging was performed on an Olympus FV1000 (Olympus America Inc., Center Valley, PA, USA) or Nikon C1 (Nikon Instruments Inc., Melville, NY, USA) confocal microscope. Images were processed with MacBiophotonic ImageJ and edited with Adobe Photoshop 7.0 (Adobe Systems Inc., San Jose, CA, USA).

Antibody Characterization

See Table 1 for a list of all primary antibodies that were used.

The anti-CD68 monoclonal antibody (Bio-Rad/AbD Serotec, clone ED1; code #MCA341GA, RRID: AB_566872) was raised in mouse using the rat ED1 protein, which is also known as rat CD68 (Cluster of Differentiation 68). This antibody recognizes a heavily

Author Manuscript Author Manuscript Author Manuscript Author Manuscript

glycosylated protein of ~90–110 kDa which is expressed on the membranes of cytoplasmic granules such as phagolysosomes, and on the cell surface of most macrophage populations and monocytes (Damoiseaux et al., 1994; Dijkstra, Dopp, Joling, & Kraal, 1985). The level of ED1 expression in a single cell can be correlated with the phagocytic activity of the respective cell type (Damoiseaux et al., 1994). We recently used this anti-CD68 antibody to show that microglia are highly phagocytic during the entire pineal gland ontogeny (Ibanez Rodriguez et al., 2016). The staining presented here matched that described in our previous report (Ibanez Rodriguez et al., 2016).

To identify microglial cells, we used two different polyclonal antibodies raised against synthetic peptides corresponding to the C-terminus of Iba1 (Ionized calcium-binding adapter molecule 1) (Ito et al., 1998). The antibodies were generated in goat (Abcam; code #ab5076, RRID: 2224402) and rabbit (Wako; code #019–19741, RRID: AB_839504). The carboxyterminal sequence of the Iba1 protein is highly conserved among human, rat and mouse. The goat anti-Iba1 antibody recognized a band at ~17 kDa on Western blots (WBs) of rat brain lysates (see manufacturer's technical information). We previously demonstrated that this antibody specifically labeled activated microglial cells in the developing and adult rat pineal gland (Ibanez Rodriguez et al., 2016). The rabbit anti-Iba1 antibody was first characterized by Imai et al. (Imai, Ibata, Ito, Ohsawa, & Kohsaka, 1996). This antibody reacted with a single ~17 kDa band on WBs using protein extracts from COS-7 cells expressing Iba1, and lysates from adult rat testis (Imai et al., 1996). Both anti-Iba1 antibodies are widely used to study microglia morphology and phagocytosis, and no cross-reactivity with neurons and astrocytes has been reported (Chen et al., 2017; Cunningham et al., 2013; Ibanez Rodriguez et al., 2016; Kanazawa, Ohsawa, Sasaki, Kohsaka, & Imai, 2002; Ohsawa, Imai, Kanazawa, Sasaki, & Kohsaka, 2000; Thion et al., 2018). Similar staining pattern was observed for both anti-Iba1 antibodies, and it matched that described in previous reports.

The essential transcription factor Pax6 (Paired box 6) was identified using two different antibodies. The mouse monoclonal anti-Pax6 antibody (Abcam; code #ab78545, RRID: AB_1566562) was raised against the recombinant full length protein corresponding to human PAX6. The rabbit polyclonal anti-Pax6 antibody (BioLegend, code #901301, RRID: AB_2565003; Covance, code #PRB-278P, RRID: AB_291612) was generated against a peptide derived from the C-terminus of the mouse Pax6 protein (amino acids QVPGSEPDMSQYWPRLQ). This sequence is conserved in rat. The monoclonal antibody recognizes both products of the two major alternatively spliced forms (Walther & Gruss, 1991), in a tissue-specific manner (see manufacturer's technical information). This antibody reacted with PAX6 on WBs of protein extracts from two human retinoblastoma cell lines, SO-Rb50 and Y79 (Meng, Wang, & Li, 2014). The polyclonal antibody was initially characterized by Davis and Reed (Davis & Reed, 1996). This antibody detected two closely migrating bands of ~50 kDa on SDS polyacrylamide gels of protein extracts from adult mouse tissues, including brain, olfactory bulb, eye, and olfactory turbinates, but not from liver. The protein doublet corresponds to the sizes predicted for the alternative spliced variants of Pax6 (Walther & Gruss, 1991). The nuclear pattern described here for Pax6 was similar for both antisera, and it matched that of our previous reports in the cerebral cortex and the pineal gland (Cunningham et al., 2013; Ibanez Rodriguez et al., 2016; Martínez-

Author Manuscript Author Manuscript Author Manuscript Author Manuscript

Cerdeno et al., 2016), as well as other work from unrelated laboratories (Davis & Reed, 1996; Del Toro et al., 2017).

The expression pattern of PCNA (Proliferating Cell Nuclear Antigen) was characterized using a mouse monoclonal antibody (EMB Millipore, clone PC10; code #MAB424, RRID: AB_95106) raised against the rat PCNA made in the protein A vector pR1T2T. The antibody was validated in IHC and WB (see manufacturer's technical information). This anti-PCNA antibody reacted strongly with a single ~36 kDa band on WBs of HeLa S100 protein fraction (Waseem & Lane, 1990). Our staining matched that obtained in cerebral cortex (Cunningham et al., 2013; Martínez-Cerdeno et al., 2016), and in our previous publication in the developing and mature rat pineal gland (Ibanez Rodriguez et al., 2016).

The mouse monoclonal anti-neuronal class III β-tubulin (Tuj1; BioLegend, code #801201 and 801202, RRID: AB_10063408; Covance, code #MMS-435P, RRID: AB_2313773) is a well-characterized antibody that was generated using microtubules from rat brain (see manufacturer's technical information). This antibody recognizes a single ~50 kDa protein band on WBs (Benitez, Castro, Patterson, Munoz, & Seltzer, 2014), and intact and degenerated nerve fibers by IHC (Hegarty, Hermes, Yang, & Aicher, 2017). We used this anti-Tuj1 antibody to stain nerve fibers in the postnatal pineal gland (Ibanez Rodriguez et al., 2016; Yu et al., 2016). Staining observed here matched that of these previous studies.

Analysis of Pax6$^+$ cells, Iba1$^+$ microglial cells and microglia-Pax6$^+$ cell interactions

Pineal gland sections were immunolabeled for Pax6 and Iba1. For samples collected after surgical procedures, we used the rabbit polyclonal anti-Pax6 combined with the goat polyclonal anti-Iba1 antibodies, and the images were captured with the Olympus FV1000 confocal microscope using a 40x objective. The proportions of total Pax6$^+$ cells, total Iba1$^+$ microglial cells, and Pax6$^+$ cells in close proximity or in the process of being phagocytosed by microglia were quantified in an area of 0.05 mm^2. For pharmacological experiments, we used both the mouse monoclonal anti-Pax6 and the rabbit polyclonal anti-Iba1 antibodies, and the images were taken with the Nikon C1 confocal microscope using a 60x objective with both cell types quantified in an area of 0.035 mm^2. The counted squares containing at least one microglia body were randomly placed in the selected images. The number of images varied among PGs (from six to ten per gland). Quantification was performed by means of the Cell Counter tool of the MacBiophotonic ImageJ software. Data were expressed as mean ± S.E.M. The statistical analysis was performed using PRISM5 (GraphPad Software Inc., La Jolla, CA, USA); one-way ANOVA followed by the Tukey post-test was performed. $P < 0.05$ was considered significant.

RESULTS

To define the plasticity and dynamics of microglia under adverse conditions in the adult pineal gland, we challenged the cells via surgical and pharmacological treatments. First, we disrupted the sympathetic innervation by performing bilateral superior cervical ganglionectomy (SCGx) (Savastano et al., 2010), and we then analyzed microglia density in pineal glands (PG) at 3, 6, 9 and 13 days after the surgery to delineate the response of pineal microglia to SCGx. Control animals were sacrificed at the same time points after sham

Author Manuscript Author Manuscript Author Manuscript Author Manuscript

surgery. Immunolabeling of pineal gland sections for the microglial marker Iba1 and subsequent quantitative analysis revealed that SCGx induced a significant increase in the density of Iba1$^+$ cells by 3 days after surgery. The increased number of microglia was observed for 9 days, returning to the sham baseline value 13 days after SCGx (Figure 1). As expected, bilateral SCGx caused Wallerian degeneration (WD) of sympathetic nerve fibers positive for the neuronal class III β-tubulin (Tuj1) within the pineal gland (Figures 2, 3 and 4). We observed nerve fiber fragmentation through 13 days after SCGx. Conversely, a densely packed innervation was observed in the PG from sham-operated animals (Figures 2 and 3). Double immunostaining for Tuj1 and Iba1 showed microglial cells in close association with degenerated fibers in the SCGx PGs (Figures 3 and 4).

We next performed experiments that included a third group subjected to bilateral decentralization of the SCG (SCGd), in addition to the SCGx and sham-operated animals. SCGd surgery disrupts the sympathetic innervation to the pineal gland by removal of 2 to 3 mm of both sympathetic trunks, but keeps the SCG and efferent nerve connections to the pineal gland intact (Hartley et al., 2015; Savastano et al., 2010). Animals from the three groups were euthanized 4 days after surgeries. We analyzed sympathetic nerve fibers in the pineal gland using the neuronal marker Tuj1. In both control and SCGd groups, we observed intact nerve fibers (Figure 5a, d, g and Figure 5b, e, h, respectively). In contrast, WD and microglia-fragmented fiber associations were evident in SCGx pineal glands 4 days after surgery (Figure 5c, f, i). Despite differences in nerve fiber degeneration, our morphometric analysis revealed that the density of Iba1$^+$ microglial cells was significantly higher in the pineal glands of both SCGx and SCGd groups compared to controls, with the majority of the microglia located in cell clusters (Figures 6 and 7a). The number of microglial cells in the SCGx and SCGd groups, however, did not significantly differ from one another (Figure 7a).

We recently showed that Pax6$^+$ cells in the adult pineal gland appear to derive from Pax6$^+$/Vimentin$^+$ neuroepithelial precursor cells in the pineal primordium, and are closely affiliated with and phagocytosed by microglia (Ibanez Rodriguez et al., 2016). We therefore evaluated the impact of superior cervical ganglionectomy and decentralization of both SCG on the Pax6$^+$ cell population. We paid special attention to cellular interactions between microglia and Pax6$^+$ cells after SCGx and SCGd surgeries. Four days after surgical stimuli, the number of Pax6$^+$ cells per area increased in both SCGd and SCGx PGs compared to control glands, but the increase was significant only in the SCGx group (Figures 6 and 7b). Similar results were observed when the association between microglia and Pax6$^+$ cells was analyzed. The percentage of Pax6$^+$ cells that were contacted by and/or engulfed by microglia was higher in both experimental groups, but this difference was significant only in the SCGx group (Figures 6c, f, i, l-o and 7c).

To determine if the difference in Iba1$^+$ and Pax6$^+$ cell density was due to self-renewal, we coimmunostained pineal gland sections with the mitotic cell marker PCNA, together with either Iba1 or Pax6. Four days after either SCGx or SCGd, the majority of Iba1-immunoreactive microglial cells were highly positive for PCNA (Figure 8). In contrast, Pax6$^+$ cells were mostly negative for PCNA (Pax6$^+$/PCNA$^-$ cells), although a few Pax6^{high}/PCNA^{low} cells were observed in each group (See white arrowheads in Figure 9).

Author Manuscript Author Manuscript Author Manuscript Author Manuscript

Our previous report showed that pineal microglia are highly phagocytic in the normal adult pineal gland (Ibanez Rodriguez et al., 2016). Therefore, we determined whether the increased microglial cell density following SCGx or SCGd was accompanied by an enhanced phagocytic capacity. For this, we included the lysosomal marker ED1 (CD68) in our IHC assays (Figure 10). The majority of $Iba1^+$ microglial cells expressed ED1 in each group, with apparent intercellular heterogeneity. Nevertheless, we found that the number and size of the ED1-positive cytoplasmic bodies per microglial cell were increased after either SCGx or SCGd. This is consistent with the idea that phagocytic capacity was potentiated by impairing sympathetic signaling to the pineal gland via ganglionectomy or decentralization.

We next pharmacologically challenged pineal microglial cells by treating adult male rats with either bacterial lipopolysaccharides (LPS) or the antibiotic doxycycline (DOX), in order to activate or inhibit microglial function, respectively. These trials consisted of three groups: control animals received vehicle for seven days; the DOX group was treated intraperitoneally (IP) with 45 mg per kg of body weight for seven days, and the LPS group received two sequential injections of 100 μg/kg of body weight, IP, once per day. Animals were sacrificed 24 hours after the last drug administration. Morphometric analysis showed that the number of $Iba1^+$ microglial cells per area increased more than twofold after LPS administration compared to the control and DOX groups, and that microglial cells were arranged in large cell clusters in the pineal glands of LPS-treated animals (Figures 11 and 12a). DOX treatment did not affect the density or distribution of $Iba1^+$ cells. In contrast to SCGx stimulus, the number of $Pax6^+$ cells per area did not vary with the pharmacological treatments (Figures 11 and 12b). However, the percentage of $Pax6^+$ cells contacted by and/or apparently phagocytosed by pineal microglia was significantly increased after LPS administration compared to control and DOX groups (Figures 11 and 12c). The DOX antibiotic did not affect the frequency of cellular interaction events between microglia and $Pax6^+$ cells. Interestingly, we found that individual microglial cells contacted multiple $Pax6^+$ cells at the same time in the LPS-treated group (Figure 13), a phenomenon we also observed in the SCGx PGs.

Immunostaining for PCNA showed a large increase in the number of potentially proliferative cells in the pineal gland after LPS treatment, compared to controls and animals injected with DOX (Figure 14). In the LPS-treated PG, $PCNA^+$ cells were both $Iba1^+$ and Iba1-negative, suggesting that multiple cell types responded to LPS treatment by increasing their proliferative potential (See yellow arrows and white arrowheads, respectively, in Figure 14f, i, l). However, the number of proliferative $Pax6^+$ cells in the LPS-treated PG appeared to be indistinguishable from controls, as most $PCNA^+/Iba1^-$ cells were also negative for Pax6 (Figure 15). A few $Pax6^{high}/PCNA^{high}$ cells and $Pax6^{high}/PCNA^{low}$ cells were observed in the experimental groups (See yellow arrowheads and white arrowheads, respectively, in Figure 15).

Finally, we analyzed ED1 expression in the adult rat pineal gland after LPS or DOX treatment. The expression of ED1 was potentiated by LPS administration. Microglial cells with numerous and heterogeneous $ED1^+$ cytoplasmic bodies were observed in LPS-treated PGs (Figures 16 and 17). We found no difference in the ED1 expression pattern between control and DOX groups.

Author Manuscript Author Manuscript Author Manuscript Author Manuscript

DISCUSSION

We recently showed that microglia are constantly ‘activated’ throughout the whole ontogeny of the pineal gland, and that microglial cells regulate pineal development and function by association and interaction with $Pax6^+$ cells and signaling elements such as pinealocyte neurites, blood vessels, and sympathetic nerve fibers (Ibanez Rodriguez et al., 2016). Association and apparent phagocytosis of $Pax6^+$ cells by highly phagocytic and proliferative microglial cells ($Iba1^+/PCNA^+/ED1^+$ cells) were observed mainly in the healthy adult pineal gland (PG). The $Pax6^+$ cells in the mature gland may derive from $Pax6^+/Vimentin^+$ neuroepithelial precursor cells which are thought to give rise to both pinealocyte and astrocyte-like glial lineages during pineal ontogeny.

Here, we studied the capacity of the pineal microglia to sense and respond to different adverse conditions. We challenged the microglia in the adult pineal gland via surgical and pharmacological stimuli, and we analyzed microglial states and interactions between microglia and $Pax6^+$ cells by quantitative immunohistochemistry.

First, we challenged the pineal microglia by bilateral surgical removal of the superior cervical ganglia (SCGx), which leads to an irreversible sympathetic denervation of the pineal gland and suppression of the circadian melatonin rhythm and other noradrenaline-dependent oscillatory events (Bailey et al., 2009; Castro et al., 2015; Savastano et al., 2010). SCGx results in Wallerian degeneration (WD) of the sympathetic nerve fibers with a transient supraliminal release of noradrenaline during the acute phase (10–30 hours after surgery) (Savastano et al., 2010). WD is a highly regulated process observed in any axonal injury due to diverse etiologies (Coleman & Freeman, 2010), and is characterized by a progressive degeneration and fragmentation of the axonal cytoskeleton and tissue envelopes from the distal ends, and a subsequent recruitment of phagocytes among other cell types (Sato et al., 2015). Interestingly, WD in the central nervous system (CNS) has been found to be slower and incomplete compared to that in the peripheral nervous system (PNS) (Coleman & Freeman, 2010; Vargas & Barres, 2007). In this study, we immunolabeled pineal gland sections for the neuronal class III β-tubulin (Tuj1) and as expected, we observed nerve fiber fragmentation after SCGx (Figures 2, 3, 4 and 5). Conversely, a densely packed innervation was observed in the PG from sham-operated animals (Figures 2, 3 and 5). We also immunostained pineal microglia using a specific antibody against the ionized Ca^{2+}-binding adapter molecule 1 (Iba1), in order to study the response of the local phagocytes to SCGx. Microglial cell density increased significantly 3 days after surgery and stayed at high levels for 9 days. SCGx-induced microgliosis was resolved by 13 days after SCG removal (Figure 1). In the SCGx PG, microglial cells were arranged in clusters that were closely associated with degenerated nerve fibers and also with intact non-sympathetic fibers (Moller & Baeres, 2002; Simonneaux & Ribelayga, 2003) (Figures 3, 4 and 5). Phagocytosis of nerve fibers by microglial cells was observed more frequently after SCGx.

Immunolabeling for Tuj1 also confirmed that the denervation of the pineal gland by decentralization of both SCG (SCGd) did not cause WD of the sympathetic nerve fibers within the pineal gland (Figure 5). Therefore, noradrenaline re-uptake and other events that depend on the integrity of sympathetic nerve endings in the pineal gland appeared not to be

Author Manuscript Author Manuscript Author Manuscript Author Manuscript

affected (Hartley et al., 2015). Despite differences in sympathetic nerve degeneration, the density of proliferative microglial cells with enhanced phagocytic potential ($Iba1^+$/$PCNA^+$/$ED1^+$ cells) increased significantly 4 days after the SCGd, reaching values comparable with those observed 4 days after SCGx (Figures 6, 7a, 8 and 10). This similar response could be explained by post-traumatic stress and the effects of circulating catecholamines and glucocorticoids on pineal microglia via specific receptors (da Silveira Cruz-Machado et al., 2017; Walker et al., 2013). SCGd-induced microgliosis suggests that microglia in the PG are also capable of sensing and responding to subtle changes in the local sympathetic innervation. This is consistent with the concept that microglia have the capacity to influence neural circuit formation and maintenance in both health and neurodegeneration (Colonna & Butovsky, 2017). In the CNS, microglial cell functionality depends on neuronal activity, which implies finely tuned cross-talk between microglia and nerve fibers, dendritic spines, astrocytes, and other synaptic elements (Wake et al., 2013). Proteins of the major histocompatibility complex class I (MHC-I) and complement cascade (C1q and C3), the neuronal transmembrane glycoprotein CX3CL1, ATP, neurotransmitters, and their respective receptors (C3R; CX3CR1; purinergic, adrenergic, glutamate and GABA receptors, among others) are some of the mediators involved in neural circuit surveillance and modeling by microglia (Colonna & Butovsky, 2017; Lee, 2013). Many of these messengers have been identified in the pineal gland by global transcriptome analysis (Bailey et al., 2009; Hartley et al., 2015).

In this study, we show that SCGx and SCGd induced clustered microgliosis in the adult pineal gland 4 days after surgery (Figure 6). Further studies will be necessary to define more precisely the phenotypes and dynamics of pineal microglia following each surgery. In the SCGx PG, the influence of WD and the transient supraliminal release of noradrenaline from degenerating nerve endings, and the accumulation of circulating and neuronally released noradrenaline on microglial priming and microglia states (Gyoneva & Traynelis, 2013; Savastano et al., 2010), will also require further analysis. Understanding microglial cell turnover has been a challenge ever since the original theory of long-lived cells was supplemented by the current view that microglia are self-renewing even under steady-state conditions (Elmore et al., 2014; Madore, Baufeld, & Butovsky, 2017; Perry & Teeling, 2013; Tay et al., 2017). Recent work by Tay et al. (Tay et al., 2017) in the Microfetti mouse model showed that microglia self-renew stochastically in the healthy brain, but they expand in a selective clonal manner during pathology leading to clusters of daughter cells, and finally they die and migrate to resolve the resulting microgliosis and to restore the original steadystate conditions. This sequence is consistent with the kinetics of microglial cell number in the PG after SCGx (Figure 1). Like other recent studies (Gordon et al., 2014; Grabert et al., 2016), Tay et al. (Tay et al., 2017) also showed that microglia dynamics vary with the microenvironment, the brain region, and the nature of the stimulus. Self-renewal of microglia and other macrophages has not been systematically characterized in circumventricular organs (CVO), which are considered to be “the gates of the brain” (Perry & Teeling, 2013). However, our data suggest that the pineal gland could serve as an attractive model to study mechanisms of phagocyte turnover.

The assumption that the phenotypes of pineal microglia differ after SCGx or SCGd is based on our finding that only SCGx significantly increased the percentage of $Pax6^+$ cells that

Author Manuscript Author Manuscript Author Manuscript Author Manuscript

were contacted by and/or engulfed by microglial cells 4 days after surgery (Figures 6 and 7c). Although there was an increase in associations and interactions between $Pax6^+$ cells and pineal microglia, the number of $Pax6^+$ cells per area was also increased after SCGx (Figures 6 and 7b). We can speculate that this increase in the $Pax6^+$ cell density was due to an induction of self-renewal. However, a very low number of $Pax6^+$ cells were weakly immunoreactive for the mitotic cell marker PCNA in the SCGx PG at ZT6 (See white arrowheads pointing $Pax6^{hlgh}/PCNA^{low}$ cells in Figure 9). Reuter and Vollrath (Reuber & Vollrath, 1983) reported that the modest mitotic activity in the adult rat pineal, 0.2–0.6 mitosis per 1000 pinealocytes, was higher during the light phase, with inter-individual variations in the timing of peaks and troughs. $Pax6^+$ cell proliferation in the SCGx PG could therefore occur at a ZT different than ZT6. The $Pax6^+$ cell population is thought to be a latent cell reservoir in the adult PG (Ibanez Rodriguez et al., 2016; Rath et al., 2013). Like other progenitors in the injured adult brain (Dimou & Gotz, 2014; Nakatomi et al., 2002), the latency of the $Pax6^+$ cell population in the SCGx PG might be being challenged by several factors such as the lack of a functional sympathetic innervation, the transient and acute release of noradrenaline and the inflammation caused by WD, and microglia-derived signals. Out-of-phase proliferation, recruitment and migration, dedifferentiation and redifferentiation mechanisms, among others, might be involved in the increase of $Pax6^+$ cells in the SCGx PG. It seems that some of these processes overcome the enhanced phagocytic activity of the microglia and their higher affinity for the $Pax6^+$ cells after SCGx. Microglia are highly dynamic cells in terms of their capacity to interact with different cell types. Microglia not only control precursor cells but they also interact with other glial cells such as astrocytes, to influence similar pathways in the developing and adult brain (Cunningham et al., 2013; Frost & Schafer, 2016; Ibanez Rodriguez et al., 2016; Reemst et al., 2016). It is expected, therefore, that interactions between microglia and $Pax6^+$ cells affect pineal phenotype and function. A TNF/TNFR1- mediated microglia-pinealocyte network has already been proposed to modulate melatonin production under inflammatory conditions (da Silveira Cruz-Machado et al., 2012). Further studies are necessary to evaluate the involvement of the $Pax6^+$ cells in this network.

We also challenged the adult pineal microglia via intraperitoneal (IP) administration of bacterial lipopolysaccharides (LPS) and the antibiotic doxycycline (DOX) at ZT6, to induce and repress microglial activity, respectively (Cunningham et al., 2013; Jantzie et al., 2005; Lazzarini et al., 2013; Santa-Cecilia et al., 2016; Sultan et al., 2013; Yrjanheikki et al., 1998). LPS has been used extensively to trigger neuroinflammation, but the precise mechanisms and key signals involved in the propagation of the stimulus from the periphery to the CNS remain controversial (Catorce & Gevorkian, 2016; Xie et al., 2017). The pineal gland has been pointed out as an immune sensor within the brain (Markus, Cecon, & Pires-Lapa, 2013). More precisely, pineal microglia express toll-like receptor 4 (TLR4) which is triggered by pathogen-associated molecular patterns (PAMPs) such as LPS, activating the NF-κB pathway and the release of pro-inflammatory mediators including TNFα. Local and circulating TNFα transiently inhibits the transcription of the *aanat* gene, and thus the synthesis of melatonin (Carvalho-Sousa et al., 2011; da Silveira Cruz-Machado et al., 2010; da Silveira Cruz- Machado et al., 2012; Fernandes, Cecon, Markus, & Ferreira, 2006; Pontes, Cardoso, Carneiro-Sampaio, & Markus, 2007). Decreased levels of melatonin

Author Manuscript Author Manuscript Author Manuscript Author Manuscript

increase vascular permeability and colonization of the affected tissues by leucocytes (Lotufo, Lopes, Dubocovich, Farsky, & Markus, 2001; Lotufo, Yamashita, Farsky, & Markus, 2006). Given the anti-inflammatory properties of melatonin and its inhibitory effect on microglial cell activation (Chung & Han, 2003; Ding, Wang, Xu, Li, et al., 2014; Ding, Wang, Xu, Lu, et al., 2014; Min, Jang, & Kwon, 2012; Wu et al., 2011), we challenged the pineal microglia during the light phase (ZT6) to achieve a greater impact of surgical and pharmacological stimuli.

A marked microgliosis is a characteristic feature of the neuroinflammation induced by peripheral administration of LPS. In fact, Jiang-Shieh et al. (Jiang-Shieh et al., 2005) showed microgliosis and astrogliosis in the rat pineal gland 2 days after an intravenous (IV) injection of fluorescein isothiocyanate (FITC)-conjugated LPS (50 mg/kg of body weight), which also resulted in reduced levels of circulating melatonin and an enhanced immunoreactivity for serotonin in the pineal parenchyma. In this study, we also found that LPS (IP, two doses of 100 μg/kg of body weight, once per day) increased the number of pineal microglial cells per area by more than twofold 24 hrs after the last injection, compared to the control group (Figures 11 and 12a). The LPS-induced microglial cells were highly phagocytic and proliferative ($Iba1^+/PCNA^+/ED1^+$ cells), and they were arranged in clusters, like in the SCGx PGs (Figures 11, 14, 16 and 17), which also suggests a clonal expansion (Madore et al., 2017; Tay et al., 2017). The frequency of interactions and apparent phagocytosis of $Pax6^+$ cells by the pineal microglia was significantly higher 24 hrs after the last LPS injection (Figure 12c), while the density of $Pax6^+$ cells was not affected by the bacterial wall components (Figure 12b). Although the area used in the morphometric analysis of pharmacologically-challenged PGs was smaller than that considered after surgical stimuli (0.035 versus 0.05 mm^2, respectively), it is evident that the increase in the number of microglial cells and events of interactions and/or phagocytosis of $Pax6^+$ cells by microglia was more robust after LPS administration than after SCGx. LPS-induced microglia showed large accumulations of $ED1^+$ cytoplasmic bodies in both the soma and projections, a feature that is associated with an enhanced phagocytic capacity (Figures 16 and 17). Interestingly, individual microglial cells in the LPS-treated PG were able to interact with multiple $Pax6^+$ cells at the same time (Figure 13). The analysis of the proliferative potential of cells in LPS-treated PGs revealed that the microglial cell clusters were highly positive for PCNA (Figure 14). However, we also noted that some of the $PCNA^+$ cells were negative for $Iba1^+$ (See white arrowheads in Figure 14f, i, l). This led us to speculate that $PCNA^+/Iba1^-$ cells might express the transcription factor Pax6. Although a few $Pax6^+/PCNA^+$ cells were seen within the LPS-induced microglial cell clusters, their number was not sufficient to explain the increase of $PCNA^+$ cells (See arrowheads in Figure 15c, f, i). These data suggest that the inflammation induced by peripheral LPS might affect other cell populations in the PG such as recruited circulating leukocytes and their progenitors, or latent microglia precursors which were shown to be negative for Iba1 and positive for nestin and Ki67 (Elmore et al., 2014; Hughes & Bergles, 2014; Xie et al., 2017). The pineal gland as a circumventricular organ (CVO) may facilitate, therefore, the recruitment of immune cells and the propagation of a peripheral inflammation into the CNS (Vargas-Caraveo, Perez-Ishiwara, & Martínez-Martínez, 2015; Wuerfel, Infante-Duarte, Glumm, & Wuerfel, 2010).

Author Manuscript Author Manuscript Author Manuscript Author Manuscript

The fact that LPS administration significantly increased the percentage of $Pax6^+$ cells that were contacted by and/or engulfed by pineal microglia (Figure 12c), without affecting the $Pax6^+$ cell number (Figure 12b), suggests an induction of $Pax6^+$ cell turnover at a ZT different than ZT6, and a balance between self-renewal and cell elimination. These results are different from those observed in the SCGx PGs (Figure 7b, c), but are in line with those reported by Luo et al. (Luo, Koyama, & Ikegaya, 2016) in the hippocampal dentate gyrus (DG) of a mouse model of epilepsy. Those authors showed that local microglia were able to maintain the DG homeostasis by rapid removal of the excess of caspase-negative viable newborn cells induced by status epilepticus (Luo et al., 2016). The $Pax6^+$ cells engulfed by the pineal microglia after surgical and pharmacological stimuli were also negative for caspase (data not shown), suggesting alternative mechanisms of phagocytosis (Brown & Neher, 2014). The differences in the dynamics of pineal microglia between SCGx and LPS groups support the concept of heterogeneity in microglial cell responses even within the same organ (Gordon et al., 2014; Grabert et al., 2016). Cunningham et al. (Cunningham et al., 2013) reported that LPS treatment to pregnant rats (IP, single injections with 100 μg/kg of body weight at E15 and E16) produced an increase in the expression of markers associated with a neurotoxic (M1) microglial state, such as IL-1β, but did not alter morphology or number of embryonic microglial cells, when assessed three days after LPS treatment. Maternal immune activation also induced a concomitant decrease in the number of neural precursor cells (NPC) in the developing cerebral cortex. Conversely, the number of NPCs was upregulated after chronic DOX treatment (200 mg/kg in food pellet chow given *ad libitum* from E15). In this study, we show that DOX administration (IP, 45 mg/kg of body weight for 7 days) did not affect the number of microglial cells and $Pax6^+$ cells nor the frequency of interactions and associations between both cell types, at least 24 hrs after the last injection (Figures 11, 12, 14 and 16). DOX has been shown to be a potent inhibitor of microglia activity (Cunningham et al., 2013; Wang et al., 2002; Yrjanheikki et al., 1998). We do not rule out, therefore, that other non-analyzed aspects of the pineal microglia biology might have been modified by the DOX protocol applied here.

In conclusion, pineal microglial cells are a highly plastic and dynamic cell type able to sense and differentially respond to surgical and pharmacological stimuli (Figure 18). As a circumventricular organ, we propose that the pineal gland is an attractive model to study the dynamics of microglial function and the mechanisms that regulate microglial cell turnover, under normal and pathological conditions within the CNS. Global transcriptome analyses of the rodent pineal gland have shown an enrichment of messengers that mediate immune and inflammatory processes, which supports the concept that the pineal gland acts as an immunological interface between the periphery and the nervous system (Bailey et al., 2009; Hartley et al., 2015; Klein et al., 2010).

ACKNOWLEDGMENTS

We thank Jorge E. Ibanez and Julieta Scelta for technical assistance, and Raymond D. Astrue for editing the manuscript. Supported by grants from CONICET (Argentina; EM; PIPCONICET 112–201101-00247; http://www.conicet.gov.ar), ANPCyT (Argentina; EM; PICT 2012–174; PICT 2017–499; http://www.agencia.mincyt.gob.ar), NIH (USA; SN; RO1 MH101188; https://www.nih.gov), and NIH-CONICET (EM and SN; F65096; 2017–2019).

Author Manuscript Author Manuscript Author Manuscript Author Manuscript

REFERENCES

Ajmone-Cat MA, Mancini M, De Simone R, Cilli P, & Minghetti L (2013). Microglial polarization and plasticity: evidence from organotypic hippocampal slice cultures. Glia, 61(10), 1698–1711. doi: 10.1002/glia.22550 [PubMed: 23918452]

Ajmone-Cat MA, Nicolini A, & Minghetti L (2003). Prolonged exposure of microglia to lipopolysaccharide modifies the intracellular signaling pathways and selectively promotes prostaglandin E2 synthesis. J Neurochem, 87(5), 1193–1203. [PubMed: 14622099]

Bailey MJ, Coon SL, Carter DA, Humphries A, Kim JS, Shi Q, . . . Klein DC (2009). Night/day changes in pineal expression of >600 genes: central role of adrenergic/cAMP signaling. J Biol Chem, 284(12), 7606–7622. doi:10.1074/jbc.M808394200 [PubMed: 19103603]

Benitez SG, Castro AE, Patterson SI, Muñoz EM, & Seltzer AM (2014). Hypoxic preconditioning differentially affects GABAergic and glutamatergic neuronal cells in the injured cerebellum of the neonatal rat. PLoS One, 9(7), e102056. doi:10.1371/journal.pone.0102056 [PubMed: 25032984]

Brown GC, & Neher JJ (2014). Microglial phagocytosis of live neurons. Nat Rev Neurosci, 15(4), 209–216. doi:10.1038/nrn3710 [PubMed: 24646669]

Cacci E, Ajmone-Cat MA, Anelli T, Biagioni S, & Minghetti L (2008). In vitro neuronal and glial differentiation from embryonic or adult neural precursor cells are differently affected by chronic or acute activation of microglia. Glia, 56(4), 412–425. doi:10.1002/glia.20616 [PubMed: 18186084]

Carvalho-Sousa CE, da Silveira Cruz-Machado S, Tamura EK, Fernandes PA, Pinato L, Muxel SM, . . . Markus RP (2011). Molecular basis for defining the pineal gland and pinealocytes as targets for tumor necrosis factor. Front Endocrinol (Lausanne), 2, 10. doi:10.3389/fendo.2011.00010 [PubMed: 22654792]

Castro AE, Benitez SG, Farias Altamirano LE, Savastano LE, Patterson SI, & Munoz EM (2015). Expression and cellular localization of the transcription factor NeuroD1 in the developing and adult rat pineal gland. J Pineal Res, 58(4), 439–451. doi:10.1111/jpi.12228 [PubMed: 25752781]

Catorce MN, & Gevorkian G (2016). LPS-induced Murine Neuroinflammation Model: Main Features and Suitability for Pre-clinical Assessment of Nutraceuticals. Curr Neuropharmacol, 14(2), 155–164. [PubMed: 26639457]

Chen KS, Harris L, Lim JWC, Harvey TJ, Piper M, Gronostajski RM, . . . Bunt J (2017). Differential neuronal and glial expression of nuclear factor I proteins in the cerebral cortex of adult mice. J Comp Neurol, 525(11), 2465–2483. doi:10.1002/cne.24206 [PubMed: 28295292]

Chung SY, & Han SH (2003). Melatonin attenuates kainic acid-induced hippocampal neurodegeneration and oxidative stress through microglial inhibition. J Pineal Res, 34(2), 95–102. [PubMed: 12562500]

Coleman MP, & Freeman MR (2010). Wallerian degeneration, wld(s), and nmnat. Annu Rev Neurosci, 33, 245–267. doi:10.1146/annurev-neuro-060909-153248 [PubMed: 20345246]

Colonna M, & Butovsky O (2017). Microglia Function in the Central Nervous System During Health and Neurodegeneration. Annu Rev Immunol, 35, 441–468. doi:10.1146/annurev-immunol-051116-052358 [PubMed: 28226226]

Cunningham CL, Martínez-Cerdeno V, & Noctor SC (2013). Microglia regulate the number of neural precursor cells in the developing cerebral cortex. J Neurosci, 33(10), 4216–4233. doi:10.1523/JNEUROSCI.3441-12.2013 [PubMed: 23467340]

da Silveira Cruz-Machado S, Carvalho-Sousa CE, Tamura EK, Pinato L, Cecon E, Fernandes PA, . . . Markus RP (2010). TLR4 and CD14 receptors expressed in rat pineal gland trigger NFKB pathway. J Pineal Res, 49(2), 183–192. doi:10.1111/j.1600-079X.2010.00785.x [PubMed: 20586888]

da Silveira Cruz-Machado S, Pinato L, Tamura EK, Carvalho-Sousa CE, & Markus RP (2012). Glia-pinealocyte network: the paracrine modulation of melatonin synthesis by tumor necrosis factor (TNF). PLoS One, 7(7), e40142. doi:10.1371/journal.pone.0040142 [PubMed: 22768337]

da Silveira Cruz-Machado S, Tamura EK, Carvalho-Sousa CE, Rocha VA, Pinato L, Fernandes PAC, & Markus RP (2017). Daily corticosterone rhythm modulates pineal function through NFkappaB-related gene transcriptional program. Sci Rep, 7(1), 2091. doi:10.1038/s41598-017-02286-y [PubMed: 28522814]

Author Manuscript Author Manuscript Author Manuscript Author Manuscript

Damoiseaux JG, Dopp EA, Calame W, Chao D, MacPherson GG, & Dijkstra CD (1994). Rat macrophage lysosomal membrane antigen recognized by monoclonal antibody ED1. Immunology, 83(1), 140–147. [PubMed: 7821959]

Davis JA, & Reed RR (1996). Role of Olf-1 and Pax-6 transcription factors in neurodevelopment. J Neurosci, 16(16), 5082–5094. [PubMed: 8756438]

Del Toro D, Ruff T, Cederfjall E, Villalba A, Seyit-Bremer G, Borrell V, & Klein R (2017). Regulation of Cerebral Cortex Folding by Controlling Neuronal Migration via FLRT Adhesion Molecules. Cell, 169(4), 621–635 e616. doi:10.1016/j.cell.2017.04.012 [PubMed: 28475893]

Dijkstra CD, Dopp EA, Joling P, & Kraal G (1985). The heterogeneity of mononuclear phagocytes in lymphoid organs: distinct macrophage subpopulations in rat recognized by monoclonal antibodies ED1, ED2 and ED3. Adv Exp Med Biol, 186, 409–419. [PubMed: 4050587]

Dimou L, & Gotz M (2014). Glial cells as progenitors and stem cells: new roles in the healthy and diseased brain. Physiol Rev, 94(3), 709–737. doi:10.1152/physrev.00036.2013 [PubMed: 24987003]

Ding K, Wang H, Xu J, Li T, Zhang L, Ding Y, . . . Zhou M (2014). Melatonin stimulates antioxidant enzymes and reduces oxidative stress in experimental traumatic brain injury: the Nrf2-ARE signaling pathway as a potential mechanism. Free Radic Biol Med, 73, 1–11. doi:10.1016/j.freeradbiomed.2014.04.031 [PubMed: 24810171]

Ding K, Wang H, Xu J, Lu X, Zhang L, & Zhu L (2014). Melatonin reduced microglial activation and alleviated neuroinflammation induced neuron degeneration in experimental traumatic brain injury: Possible involvement of mTOR pathway. Neurochem Int, 76, 23–31. doi:10.1016/j.neuint.2014.06.015 [PubMed: 24995391]

Ekdahl CT, Kokaia Z, & Lindvall O (2009). Brain inflammation and adult neurogenesis: the dual role of microglia. Neuroscience, 158(3), 1021–1029. doi:10.1016/j.neuroscience.2008.06.052 [PubMed: 18662748]

Elmore MR, Najafi AR, Koike MA, Dagher NN, Spangenberg EE, Rice RA, . . . Green KN (2014). Colony-stimulating factor 1 receptor signaling is necessary for microglia viability, unmasking a microglia progenitor cell in the adult brain. Neuron, 82(2), 380–397. doi:10.1016/j.neuron.2014.02.040 [PubMed: 24742461]

Fernandes PA, Cecon E, Markus RP, & Ferreira ZS (2006). Effect of TNF-alpha on the melatonin synthetic pathway in the rat pineal gland: basis for a ‘feedback’ of the immune response on circadian timing. J Pineal Res,; 41(4), 344–350. doi:10.1111/j.1600-079X.2006.00373.x [PubMed: 17014691]

Frost JL, & Schafer DP (2016). Microglia: Architects of the Developing Nervous System. Trends Cell Biol. doi:10.1016/j.tcb.2016.02.006

Gordon S, Pluddemann A, & Martínez Estrada F (2014). Macrophage heterogeneity in tissues: phenotypic diversity and functions. Immunol Rev, 262(1), 36–55. doi:10.1111/imr.12223 [PubMed: 25319326]

Grabert K, Michoel T, Karavolos MH, Clohisey S, Baillie JK, Stevens MP, . . . McColl BW (2016). Microglial brain region-dependent diversity and selective regional sensitivities to aging. Nat Neurosci, 19(3), 504–516. doi:10.1038/nn.4222 [PubMed: 26780511]

Gyoneva S, & Traynelis SF (2013). Norepinephrine modulates the motility of resting and activated microglia via different adrenergic receptors. J Biol Chem, 288(21), 15291–15302. doi:10.1074/jbc.M113.458901 [PubMed: 23548902]

Hartley SW, Coon SL, Savastano LE, Mullikin JC, Program, Nisc Comparative Sequencing, Fu, C., & Klein, D. C. (2015). Neurotranscriptomics: The Effects of Neonatal Stimulus Deprivation on the Rat Pineal Transcriptome. PLoS One, 10(9), e0137548. doi:10.1371/journal.pone.0137548 [PubMed: 26367423]

Hegarty DM, Hermes SM, Yang K, & Aicher SA (2017). Select noxious stimuli induce changes on corneal nerve morphology. J Comp Neurol, 525(8), 2019–2031. doi:10.1002/cne.24191 [PubMed: 28213947]

Hughes EG, & Bergles DE (2014). Hidden progenitors replace microglia in the adult brain. Neuron, 82(2), 253–255. doi:10.1016/j.neuron.2014.04.010 [PubMed: 24742453]

Author Manuscript Author Manuscript Author Manuscript Author Manuscript

Ibanez Rodriguez MP, Noctor SC, & Muñoz EM (2016). Cellular Basis of Pineal Gland Development: Emerging Role of Microglia as Phenotype Regulator. PLoS One, 11(11), e0167063. doi:10.1371/journal.pone.0167063 [PubMed: 27861587]

Imai Y, Ibata I, Ito D, Ohsawa K, & Kohsaka S (1996). A novel gene iba1 in the major histocompatibility complex class III region encoding an EF hand protein expressed in a monocytic lineage. Biochem Biophys Res Commun, 224(3), 855–862.doi:10.1006/bbrc.1996.1112 [PubMed: 8713135]

Ito D, Imai Y, Ohsawa K, Nakajima K, Fukuuchi Y, & Kohsaka S (1998). Microglia-specific localisation of a novel calcium binding protein, Iba1. Brain Res Mol Brain Res, 57(1), 1–9. [PubMed: 9630473]

Jantzie LL, Cheung PY, & Todd KG (2005). Doxycycline reduces cleaved caspase-3 and microglial activation in an animal model of neonatal hypoxia-ischemia. J Cereb Blood Flow Metab, 25(3), 314–324. doi:10.1038/sj.jcbfm.9600025 [PubMed: 15647741]

Jiang-Shieh YF, Wu CH, Chien HF, Wei IH, Chang ML, Shieh JY, & Wen CY (2005). Reactive changes of interstitial glia and pinealocytes in the rat pineal gland challenged with cell wall components from gram-positive and -negative bacteria. J Pineal Res, 38(1), 17–26. doi:10.1111/j.1600-079X.2004.00170.x [PubMed: 15617533]

Kanazawa H, Ohsawa K, Sasaki Y, Kohsaka S, & Imai Y (2002). Macrophage/microglia-specific protein Iba1 enhances membrane ruffling and Rac activation via phospholipase C-gamma -dependent pathway. J Biol Chem, 277(22), 20026–20032. doi:10.1074/jbc.M109218200 [PubMed: 11916959]

Kettenmann H, Hanisch UK, Noda M, & Verkhratsky A (2011). Physiology of microglia. Physiol Rev, 91(2), 461–553. doi:10.H52/physrev.00011.2010 [PubMed: 21527731]

Kigerl KA, Gensel JC, Ankeny DP, Alexander JK, Donnelly DJ, & Popovich PG (2009). Identification of two distinct macrophage subsets with divergent effects causing either neurotoxicity or regeneration in the injured mouse spinal cord. J Neurosci, 29(43), 13435–13444. doi:10.1523/JNEUROSCI.3257-09.2009 [PubMed: 19864556]

Klein DC, Bailey MJ, Carter DA, Kim JS, Shi Q, Ho AK, . . . Coon SL (2010). Pineal function: impact of microarray analysis. Mol Cell Endocrinol, 314(2), 170–183. doi:S0303–7207(09)00368–2 [pii] 10.1016/j.mce.2009.07.010 [PubMed: 19622385]

Lawson LJ, Perry VH, Dri P, & Gordon S (1990). Heterogeneity in the distribution and morphology of microglia in the normal adult mouse brain. Neuroscience, 39(1), 151–170. [PubMed: 2089275]

Lazzarini M, Martín S, Mitkovski M, Vozari RR, Stuhmer W, & Bel ED (2013). Doxycycline restrains glia and confers neuroprotection in a 6-OHDA Parkinson model. Glia, 61(7), 1084–1100. doi:10.1002/glia.22496 [PubMed: 23595698]

Lee M (2013). Neurotransmitters and microglial-mediated neuroinflammation. Curr Protein Pept Sci, 14(1), 21–32. [PubMed: 23441898]

Li L, Lu J, Tay SS, Moochhala SM, & He BP (2007). The function of microglia, either neuroprotection or neurotoxicity, is determined by the equilibrium among factors released from activated microglia in vitro. Brain Res, 1159, 8–17. doi:10.1016/j.brainres.2007.04.066 [PubMed: 17572395]

Lotufo CM, Lopes C, Dubocovich ML, Farsky SH, & Markus RP (2001). Melatonin and Nacetylserotonin inhibit leukocyte rolling and adhesion to rat microcirculation. Eur J Pharmacol, 430(2–3), 351–357. [PubMed: 11711054]

Lotufo CM, Yamashita CE, Farsky SH, & Markus RP (2006). Melatonin effect on endothelial cells reduces vascular permeability increase induced by leukotriene B4. Eur J Pharmacol, 534(1–3), 258–263. [PubMed: 16612844]

Luo C, Koyama R, & Ikegaya Y (2016). Microglia engulf viable newborn cells in the epileptic dentate gyrus. Glia, 64(9), 1508–1517. doi:10.1002/glia.23018 [PubMed: 27301702]

Madore C, Baufeld C, & Butovsky O (2017). Microglial confetti party. Nat Neurosci, 20(6), 762–763. doi:10.1038/nn.4570 [PubMed: 28542157]

Markus RP, Cecon E, & Pires-Lapa MA (2013). Immune-pineal axis: nuclear factor kappaB (NFkB) mediates the shift in the melatonin source from pinealocytes to immune competent cells. Int J Mol Sci, 14(6), 10979–10997. doi:10.3390/ijms140610979 [PubMed: 23708099]

Author Manuscript Author Manuscript Author Manuscript Author Manuscript

Martinez-Cerdeno V, Cunningham CL, Camacho J, Keiter JA, Ariza J, Lovern M, & Noctor SC (2016). Evolutionary origin of Tbr2-expressing precursor cells and the subventricular zone in the developing cortex. J Comp Neurol, 524(3), 433–447. doi:10.1002/cne.23879 [PubMed: 26267763]

Martinez FO, & Gordon S (2014). The M1 and M2 paradigm of macrophage activation: time for reassessment. F1000Prime Rep, 6, 13. doi:10.12703/P6-13 [PubMed: 24669294]

Meng B, Wang Y, & Li B (2014). Suppression of PAX6 promotes cell proliferation and inhibits apoptosis in human retinoblastoma cells. Int J Mol Med, 34(2), 399–408. doi:10.3892/ijmm.2014.1812 [PubMed: 24939714]

Min KJ, Jang JH, & Kwon TK (2012). Inhibitory effects of melatonin on the lipopolysaccharideinduced CC chemokine expression in BV2 murine microglial cells are mediated by suppression of Akt-induced NF-kappaB and STAT/GAS activity. J Pineal Res, 52(3), 296–304. doi:10.1111/j.1600-079X.2011.00943.x [PubMed: 22225513]

Moller M, & Baeres FM (2002). The anatomy and innervation of the mammalian pineal gland. Cell Tissue Res, 309(1), 139–150. doi:10.1007/s00441-002-0580-5 [PubMed: 12111544]

Moller M, Rath MF, & Klein DC (2006). The perivascular phagocyte of the mouse pineal gland: an antigen-presenting cell. Chronobiol Int, 23(1–2), 393–401. doi:10.1080/07420520500521855 [PubMed: 16687312]

Nakatomi H, Kuriu T, Okabe S, Yamamoto S, Hatano O, Kawahara N, . . . Nakafuku M (2002). Regeneration of hippocampal pyramidal neurons after ischemic brain injury by recruitment of endogenous neural progenitors. Cell, 110(4), 429–441. [PubMed: 12202033]

Ohsawa K, Imai Y, Kanazawa H, Sasaki Y, & Kohsaka S (2000). Involvement of Iba1 in membrane ruffling and phagocytosis of macrophages/microglia. J Cell Sci, 113 (Pt 17), 3073–3084. [PubMed: 10934045]

Pedersen EB, Fox LM, Castro AJ, & McNulty JA (1993). Immunocytochemical and electronmicroscopic characterization of macrophage/microglia cells and expression of class II major histocompatibility complex in the pineal gland of the rat. Cell Tissue Res, 272(2), 257–265. [PubMed: 8513480]

Pedersen EB, McNulty JA, Castro AJ, Fox LM, Zimmer J, & Finsen B (1997). Enriched immune-environment of blood-brain barrier deficient areas of normal adult rats. J Neuroimmunol, 76(1–2), 117–131. [PubMed: 9184641]

Perry VH, & Teeling J (2013). Microglia and macrophages of the central nervous system: the contribution of microglia priming and systemic inflammation to chronic neurodegeneration. Semin Immunopathol, 35(5), 601–612. doi:10.1007/s00281-013-0382-8 [PubMed: 23732506]

Pontes GN, Cardoso EC, Carneiro-Sampaio MM, & Markus RP (2007). Pineal melatonin and the innate immune response: the TNF-alpha increase after cesarean section suppresses nocturnal melatonin production. J Pineal Res, 43(4), 365–371. doi:10.1111/j.1600-079X.2007.00487.x [PubMed: 17910605]

Raivich G (2005). Like cops on the beat: the active role of resting microglia. Trends Neurosci, 28(11), 571–573. doi:10.1016/j.tins.2005.09.001 [PubMed: 16165228]

Ransohoff RM (2016). A polarizing question: do M1 and M2 microglia exist? Nat Neurosci, 19(8), 987–991. doi:10.1038/nn.4338 [PubMed: 27459405]

Rath MF, Rohde K, Klein DC, & Moller M (2013). Homeobox genes in the rodent pineal gland: roles in development and phenotype maintenance. Neurochem Res, 38(6), 1100–1112. doi:10.1007/s11064-012-0906-y [PubMed: 23076630]

Reemst K, Noctor SC, Lucassen PJ, & Hol EM (2016). The Indispensable Roles of Microglia and Astrocytes during Brain Development. Front Hum Neurosci, 10, 566. doi:10.3389/fnhum.2016.00566 [PubMed: 27877121]

Reuber H, & Vollrath L (1983). Mitotic activity and its 24-hour rhythm in the rat pineal gland. Acta Anat (Basel), 117(2), 121–127. [PubMed: 6637375]

Santa-Cecilia FV, Socias B, Ouidja MO, Sepulveda-Diaz JE, Acuna L, Silva RL, . . . Raisman- Vozari R (2016). Doxycycline Suppresses Microglial Activation by Inhibiting the p38 MAPK and NF-kB Signaling Pathways. Neurotox Res, 29(4), 447–459. doi:10.1007/s12640-015-9592- 2 [PubMed: 26745968]

Author Manuscript Author Manuscript Author Manuscript Author Manuscript

Sato F, Martínez NE, Stewart EC, Omura S, Alexander JS, & Tsunoda I (2015). “Microglial nodules” and “newly forming lesions” may be a Janus face of early MS lesions; implications from virus-induced demyelination, the Inside-Out model. BMC Neurol, 15, 219. doi:10.1186/s12883-015-0478-y [PubMed: 26499989]

Savastano LE, Castro AE, Fitt MR, Rath MF, Romeo HE, & Munoz EM (2010). A standardized surgical technique for rat superior cervical ganglionectomy. J Neurosci Methods, 192(1), 22–33. doi:10.1016/j.jneumeth.2010.07.007 [PubMed: 20637235]

Sica A, & Mantovani A (2012). Macrophage plasticity and polarization: in vivo veritas. J Clin Invest, 122(3), 787–795. doi:10.1172/JCI59643 [PubMed: 22378047]

Simonneaux V, & Ribelayga C (2003). Generation of the melatonin endocrine message in mammals: a review of the complex regulation of melatonin synthesis by norepinephrine, peptides, and other pineal transmitters. Pharmacol Rev, 55(2), 325–395. doi:10.1124/pr.55.2.2 [PubMed: 12773631]

Soulet D, & Rivest S (2008). Microglia. Curr Biol, 18(12), R506–508. doi:10.1016/j.cub.2008.04.047 [PubMed: 18579087]

Sultan S, Gebara E, & Toni N (2013). Doxycycline increases neurogenesis and reduces microglia in the adult hippocampus. Front Neurosci, 7, 131. doi:10.3389/fnins.2013.00131 [PubMed: 23898238]

Tay TL, Mai D, Dautzenberg J, Fernandez-Klett F, Lin G, Sagar, . . . Prinz M (2017). A new fate mapping system reveals context-dependent random or clonal expansion of microglia. Nat Neurosci, 20(6), 793–803. doi:10.1038/nn.4547 [PubMed: 28414331]

Thion MS, Low D, Silvin A, Chen J, Grisel P, Schulte-Schrepping J, . . . Garel S (2018). Microbiome Influences Prenatal and Adult Microglia in a Sex-Specific Manner. Cell, 172(3), 500–516 e516. doi:10.1016/j.cell.2017.11.042 [PubMed: 29275859]

Vargas-Caraveo A, Perez-Ishiwara DG, & Martínez-Martínez A (2015). Chronic Psychological Distress as an Inducer of Microglial Activation and Leukocyte Recruitment into the Area Postrema. Neuroimmunomodulation, 22(5), 311–321. doi:10.1159/000369350 [PubMed: 25765708]

Vargas ME, & Barres BA (2007). Why is Wallerian degeneration in the CNS so slow? Annu Rev Neurosci, 30, 153–179. doi:10.1146/annurev.neuro.30.051606.094354 [PubMed: 17506644]

Wake H, Moorhouse AJ, Miyamoto A, & Nabekura J (2013). Microglia: actively surveying and shaping neuronal circuit structure and function. Trends Neurosci, 36(4), 209–217. doi:10.1016/j.tins.2012.11.007 [PubMed: 23260014]

Walker FR, Nilsson M, & Jones K (2013). Acute and chronic stress-induced disturbances of microglial plasticity, phenotype and function. Curr Drug Targets, 14(11), 1262–1276. [PubMed: 24020974]

Walther C, & Gruss P (1991). Pax-6, a murine paired box gene, is expressed in the developing CNS. Development, 113(4), 1435–1449. [PubMed: 1687460]

Wang CX, Yang T, Noor R, & Shuaib A (2002). Delayed minocycline but not delayed mild hypothermia protects against embolic stroke. BMC Neurol, 2, 2. [PubMed: 11960560]

Waseem NH, & Lane DP (1990). Monoclonal antibody analysis of the proliferating cell nuclear antigen (PCNA). Structural conservation and the detection of a nucleolar form. J Cell Sci, 96 (Pt 1), 121–129. [PubMed: 1695635]

Wolf SA, Boddeke HW, & Kettenmann H (2017). Microglia in Physiology and Disease. Annu Rev Physiol, 79, 619–643. doi:10.1146/annurev-physiol-022516-034406 [PubMed: 27959620]

Wu UI, Mai FD, Sheu JN, Chen LY, Liu YT, Huang HC, & Chang HM (2011). Melatonin inhibits microglial activation, reduces pro-inflammatory cytokine levels, and rescues hippocampal neurons of adult rats with acute Klebsiella pneumoniae meningitis. J Pineal Res, 50(2), 159–170. doi:10.1111/j.1600-079X.2010.00825.x [PubMed: 21062353]

Wuerfel E, Infante-Duarte C, Glumm R, & Wuerfel JT (2010). Gadofluorine M-enhanced MRI shows involvement of circumventricular organs in neuroinflammation. J Neuroinflammation, 7, 70. doi:10.1186/1742-2094-7-70 [PubMed: 20955604]

Xie X, Luo X, Liu N, Li X, Lou F, Zheng Y, & Ren Y (2017). Monocytes, microglia, and CD200-CD200R1 signaling are essential in the transmission of inflammation from the periphery to the central nervous system. J Neurochem, 141(2), 222–235. doi:10.1111/jnc.13972 [PubMed: 28164283]

Author Manuscript Author Manuscript Author Manuscript Author Manuscript

Yrjanheikki J, Keinanen R, Pellikka M, Hokfelt T, & Koistinaho J (1998). Tetracyclines inhibit microglial activation and are neuroprotective in global brain ischemia. Proc Natl Acad Sci U S A, 95(26), 15769–15774. [PubMed: 9861045]

Yu H, Benitez SG, Jung SR, Farias Altamirano LE, Kruse M, Seo JB, . . . Hille B (2016). GABAergic signaling in the rat pineal gland. J Pineal Res. doi:10.1111/jpi.12328

Author Manuscript Author Manuscript Author Manuscript Author Manuscript

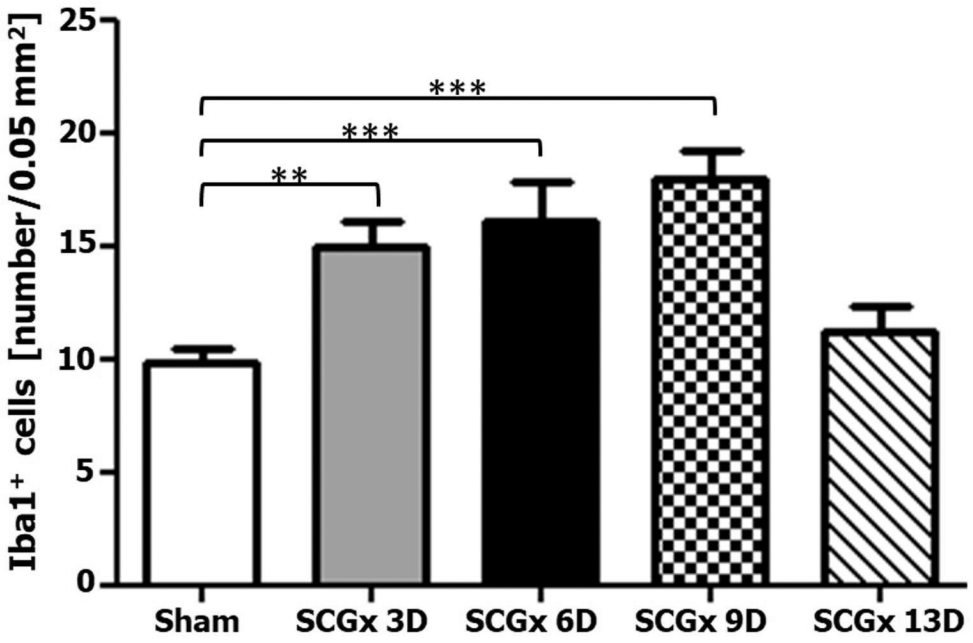

Figure 1.

Kinetics of microglial cell number in the adult rat pineal gland after bilateral superior cervical ganglionectomy (SCGx). The surgical removal of the SCG increased the number of $Iba1^+$ microglial cells per area (0.05 mm^2) in the pineal gland by 3 days (3D) after the surgery, and the density of microglia remained significantly elevated for 9 days. The number of microglial cells returned to the sham baseline level 13 days after SCGx. Three glands (N=3) per group were analyzed at each time point. Data were expressed as mean ± S.E.M. Microglia density was similar among sham-operated rats; the sham bar represents the average of the twelve control animals. Statistics: one-way ANOVA followed by the Tukey post-test; ***$P < 0.001$; **$P < 0.01$.

Author Manuscript Author Manuscript Author Manuscript Author Manuscript

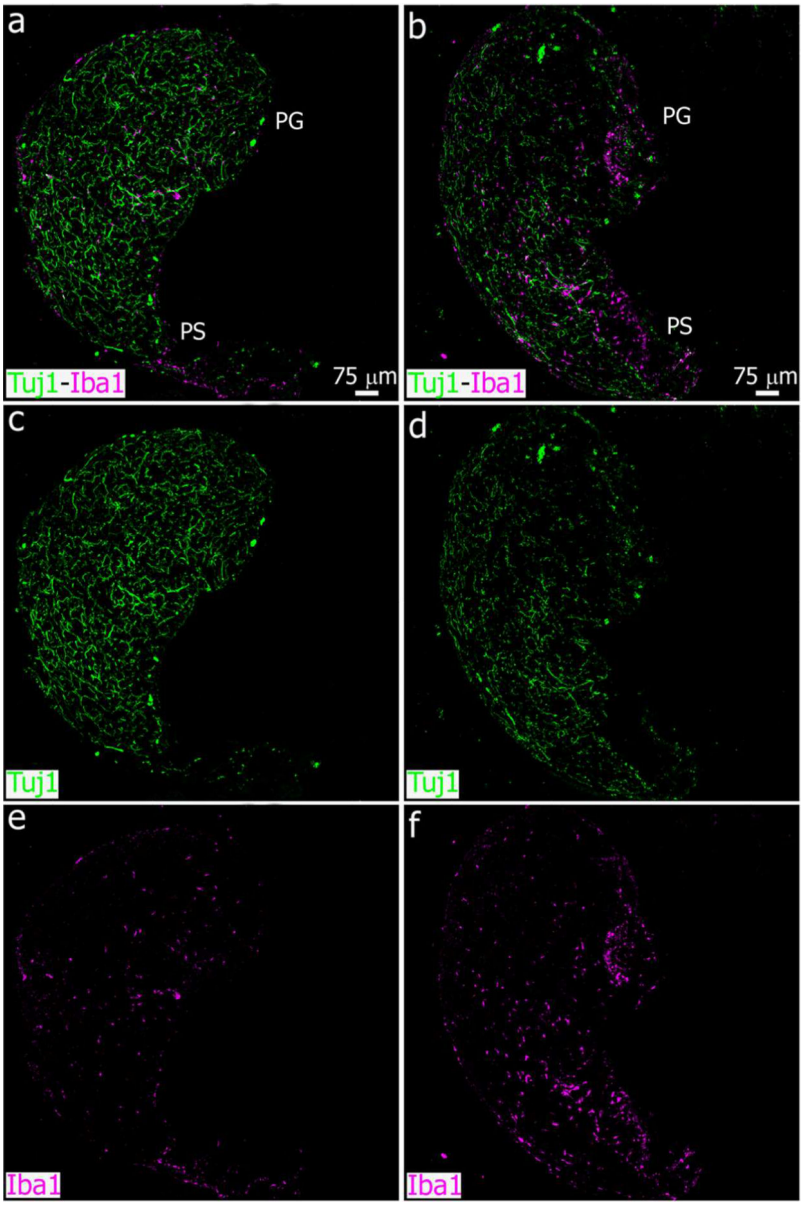

Figure 2.

Sympathetic nerve fibers degenerate and microglial cell number is increased in the adult pineal gland after bilateral SCGx. (a-f) Sections of adult pineal glands (PG) including the pineal stalk (PS), immunolabeled for the microglial marker Iba1 (magenta) and β- tubulin III (Tuj1, green) at 6 days after sham (left column, a, c, e) and SCGx surgery (right column, b, d, f). Wallerian degeneration of the sympathetic nerve fibers and a higher number of microglial cells, mainly in the proximal and ventral PG and PS, are observed in the SCGx PG compared to the control gland. (a-f) 10x; scale bar: 75 μm.

Author Manuscript Author Manuscript Author Manuscript Author Manuscript

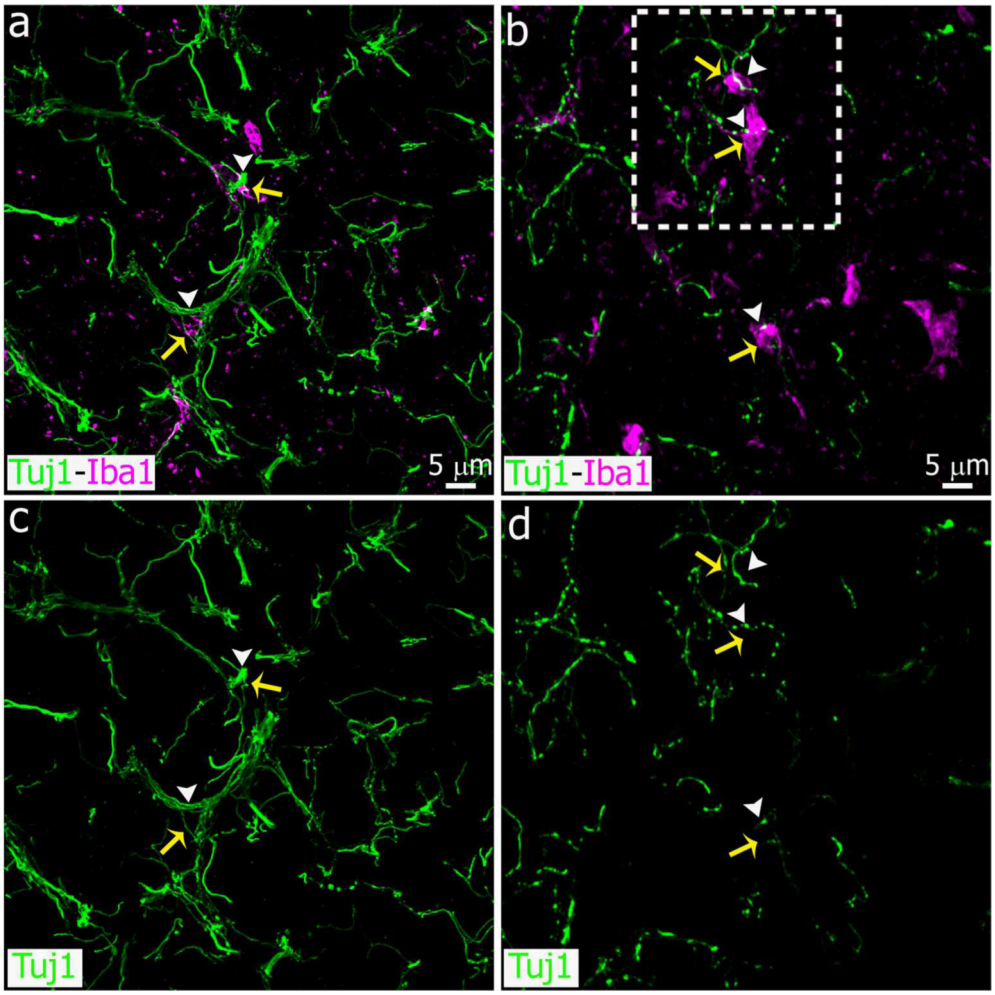

Figure 3.

Higher magnification images showing pineal microglial cells interacting and phagocytozing degenerated sympathetic nerve fibers after SCGx. Panels show microglial cells immunoreactive for Iba1 (magenta, yellow arrows) associated with normal or fragmented nerve fibers positive for Tujl (green, white arrowheads) in sham-operated (left column, a, c) and SCGx (right column, b, d) pineal glands at 6 days after surgery. Phagocytosis events were more frequent in the SCGx group. (a, c) 1.5x digital zoom from a 60x image; (b, d) 2x digital zoom from a 40x image; scale bar: 5 μm.

Author Manuscript Author Manuscript Author Manuscript Author Manuscript

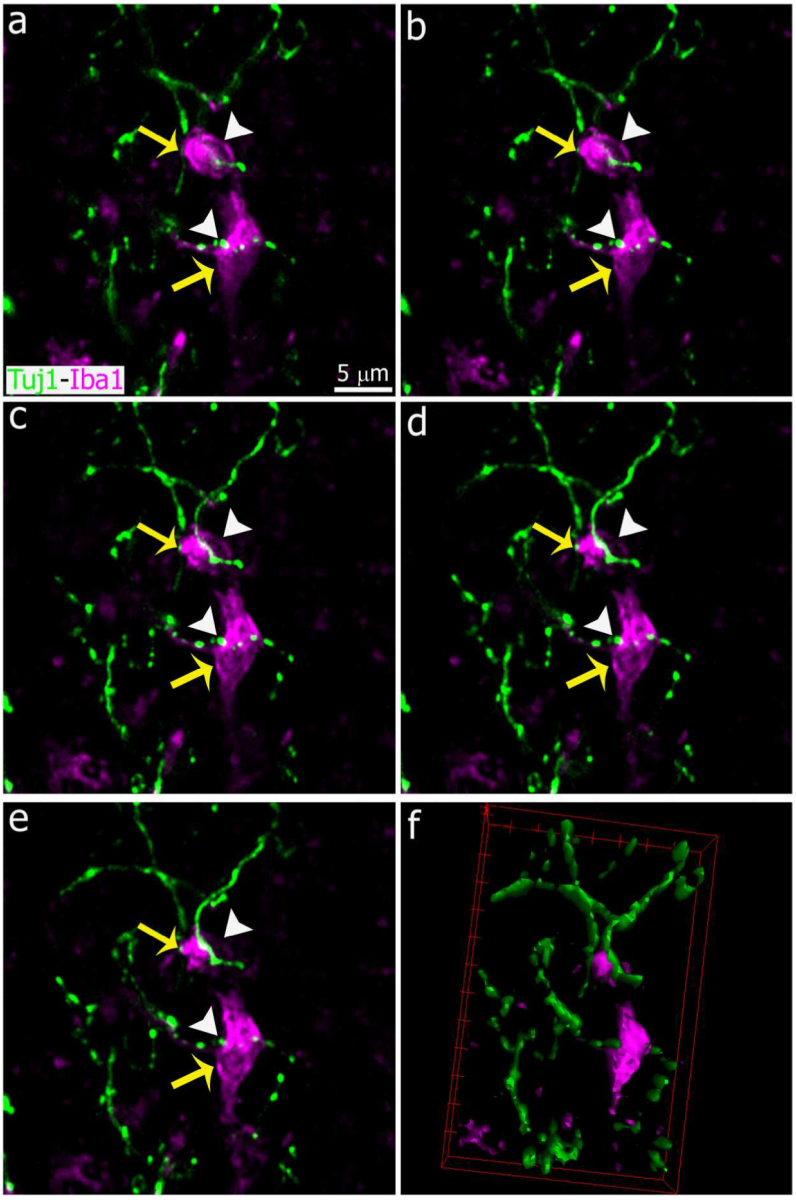

Figure 4.

Interactions between microglial cells and degenerated sympathetic nerve fibers in the pineal gland after SCGx. Images show sequential confocal planes separated by a distance of 1.5 µm (a-e) and a 3-dimensional reconstruction (f). Immunolabeling for the microglial marker Iba1 (magenta, yellow arrows) and β-tubulin III (Tuj1, green, white arrowheads). The five confocal planes displayed here were used to generate the image shown in the inset of Figure 3b. (a-e) 5x digital zoom from 40x images; scale bar: 5 µm. (f) 3-dimensional reconstruction of the five optical sections in a-e highlights interactions between microglia and fragmented nerve fibers.

Author Manuscript Author Manuscript Author Manuscript Author Manuscript

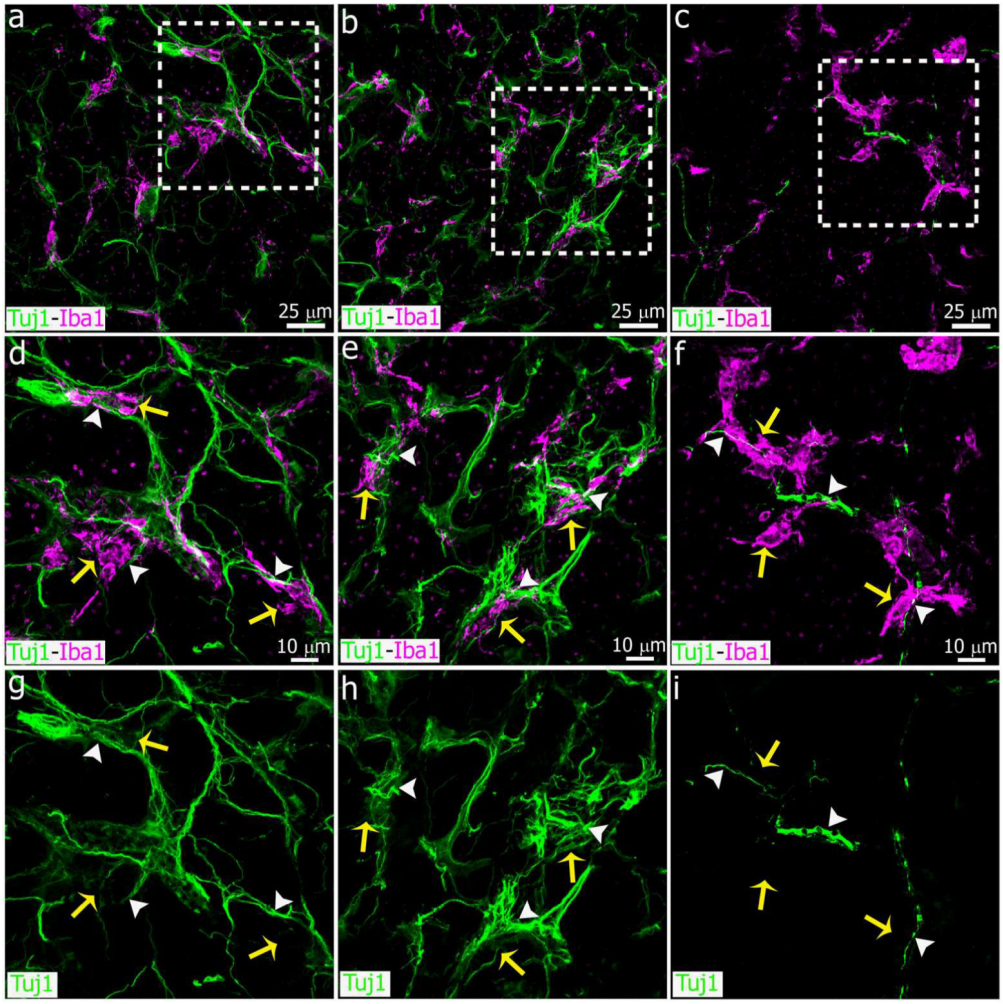

Figure 5.

Sympathetic innervation of the rat pineal gland remains intact after bilateral superior cervical decentralization (SCGd). Panels show sections of pineal glands (PG) from sham-operated (left column, a, d, g), SCGd (center column, b, e, h) and ganglionectomized (SCGx; right column, c, f, i) adult rats four days after surgery. Sections were immunostained for Iba1 (magenta) and Tuj1 (green). Wallerian degeneration was only observed after SCGx, but close association and phagocytosis of nerve fibers (white arrowheads) by microglial cells (yellow arrows) were observed in each group. (a-c) 60x; scale bar: 25 µm. (d-i) 1.8x digital zooms from the insets shown in a-c; scale bar: 10µm.

Author Manuscript Author Manuscript Author Manuscript Author Manuscript

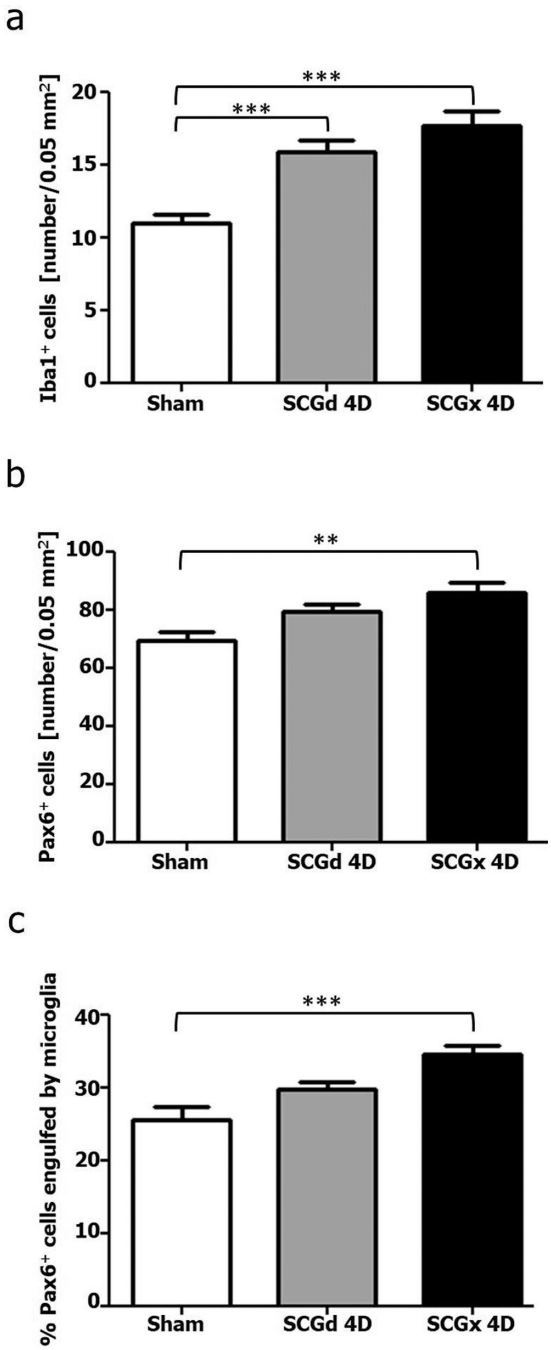

Figure 6.

Superior cervical ganglionectomy (SCGx) and decentralization of SCG (SCGd) increase microglial cell number and cellular interactions in the adult rat pineal gland. Panels show images of pineal glands (PG) immunolabeled for Iba1 (magenta, yellow arrows) and the essential transcription factor Pax6 (green, yellow arrowheads) at 4 days after sham (left column, a, d, g, j), SCGd (center column, b, e, h, k), and SCGx (right column, c, f, i, l-o) surgery. The number of Iba1$^+$ microglial cells was higher in both the SCGd and SCGx PGs compared to sham-operated animals, and microglial cell clusters were frequent in the

Author Manuscript Author Manuscript Author Manuscript Author Manuscript

experimental groups. An increase in the number of $Pax6^+$ cells, and associations between microglia and $Pax6^+$ cells were observed in the SCGx PG. Illustrative examples of microglia- $Pax6^+$ cell associations in the SCGx PG are shown in m-o. (a and c) 60x; (b) 1.5x digital zoom from a 40x image; scale bar: 25 μm. (d-l) 1.8x digital zooms from the insets shown in a-c; scale bar: 10 μm. (m-o) 5.3x digital zooms from f; scale bar: 5 μm.

Author Manuscript Author Manuscript Author Manuscript Author Manuscript

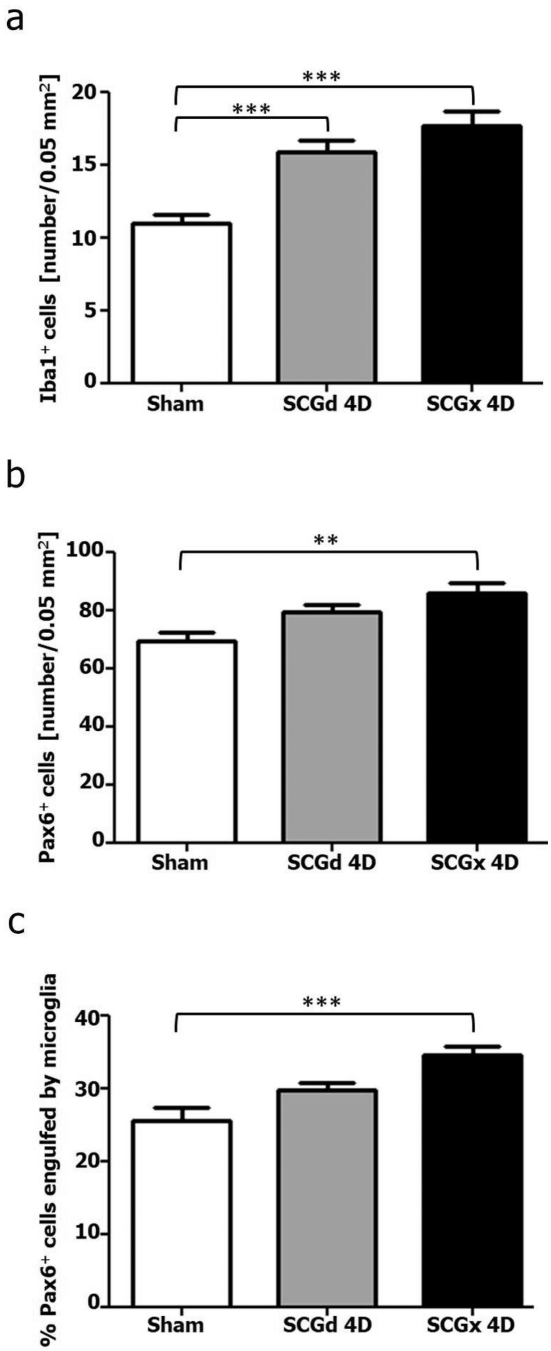

Figure 7.

Morphometric analysis of microglial cells, Pax6$^+$ cells and cellular interactions between both cell types after SCGx or SCGd. The analysis was performed 4 days (4D) after surgery, and a sham-operated group was included. (a) The number of Iba1$^+$ microglial cells per area (0.05 mm^2) increased after surgical disruption of the sympathetic innervation to the pineal gland by bilateral SCGx or SCGd. (b) The density of Pax6$^+$ cells was significantly increased in the SCGx pineal glands. (c) SCGx induced a significant increase in the percentage of Pax6$^+$ cells in contact with and/or engulfed by microglial cells. Data were expressed as

mean ± S.E.M. (N=4). Statistics: one-way ANOVA followed by the Tukey posttest; ***$P <$ 0.001; **$P <$ 0.01.

Author Manuscript Author Manuscript Author Manuscript Author Manuscript

Author Manuscript Author Manuscript Author Manuscript Author Manuscript

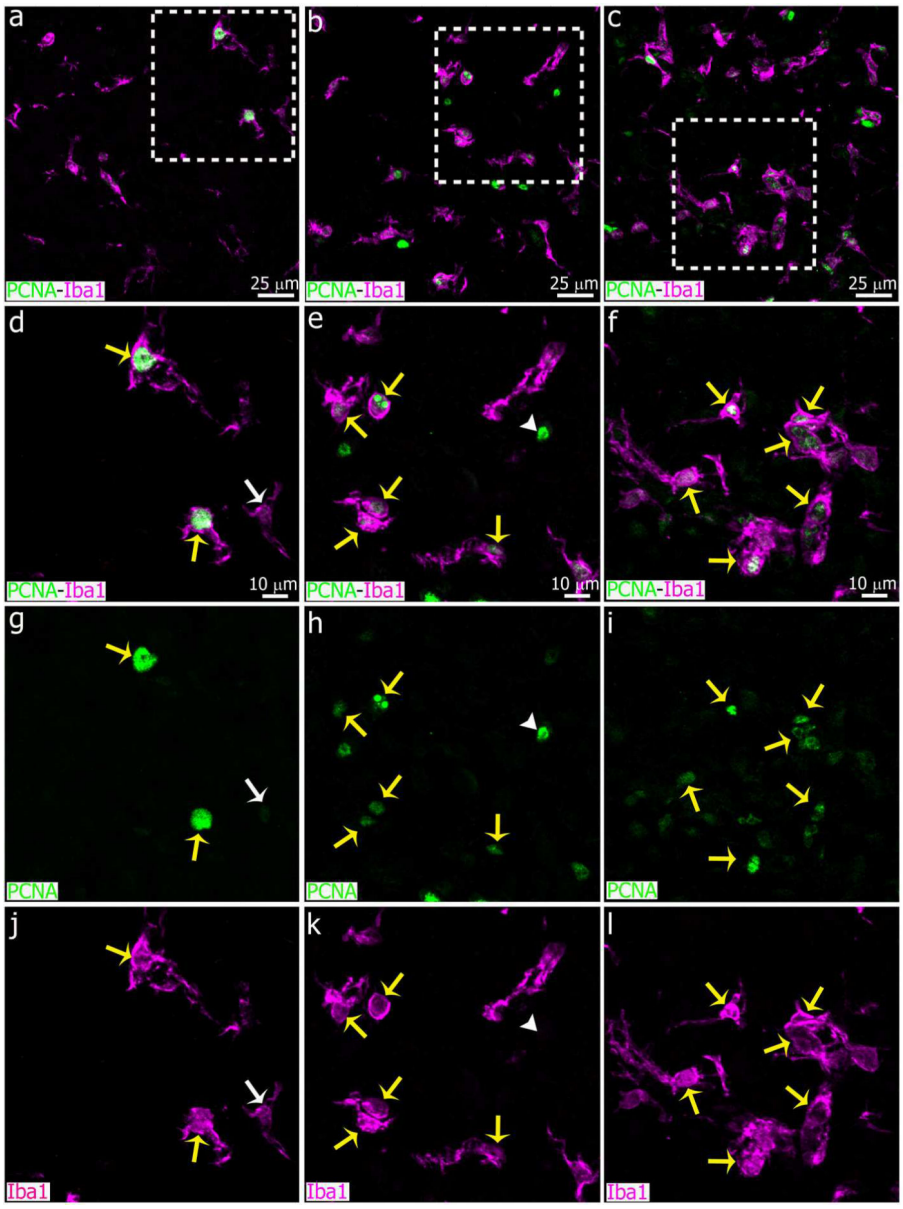

Figure 8.

The number of proliferative Iba1$^+$ microglial cells is increased in the pineal gland after SCGx or SCGd. Confocal images of adult rat pineal glands (PG) immunostained for Iba1 (magenta) and the mitotic cell marker PCNA (green) show that the majority of microglial cells are positive for both markers (yellow arrows) four days after SCGx (right column, c, f, i, l) or SCGd (center column, b, e, h, k), compared to the sham-operated group (left column, a, d, g, j). White arrows show an Iba1$^+$ cell that does not express PCNA, and white arrowheads point a PCNA$^+$ cell that does not express Iba1. (a-c) 1.5x digital zooms from 40x images; scale bar: 25 µm. (d-l) 1.9x digital zooms from the insets shown in a-c; scale bar: 10 µm.

Author Manuscript Author Manuscript Author Manuscript Author Manuscript

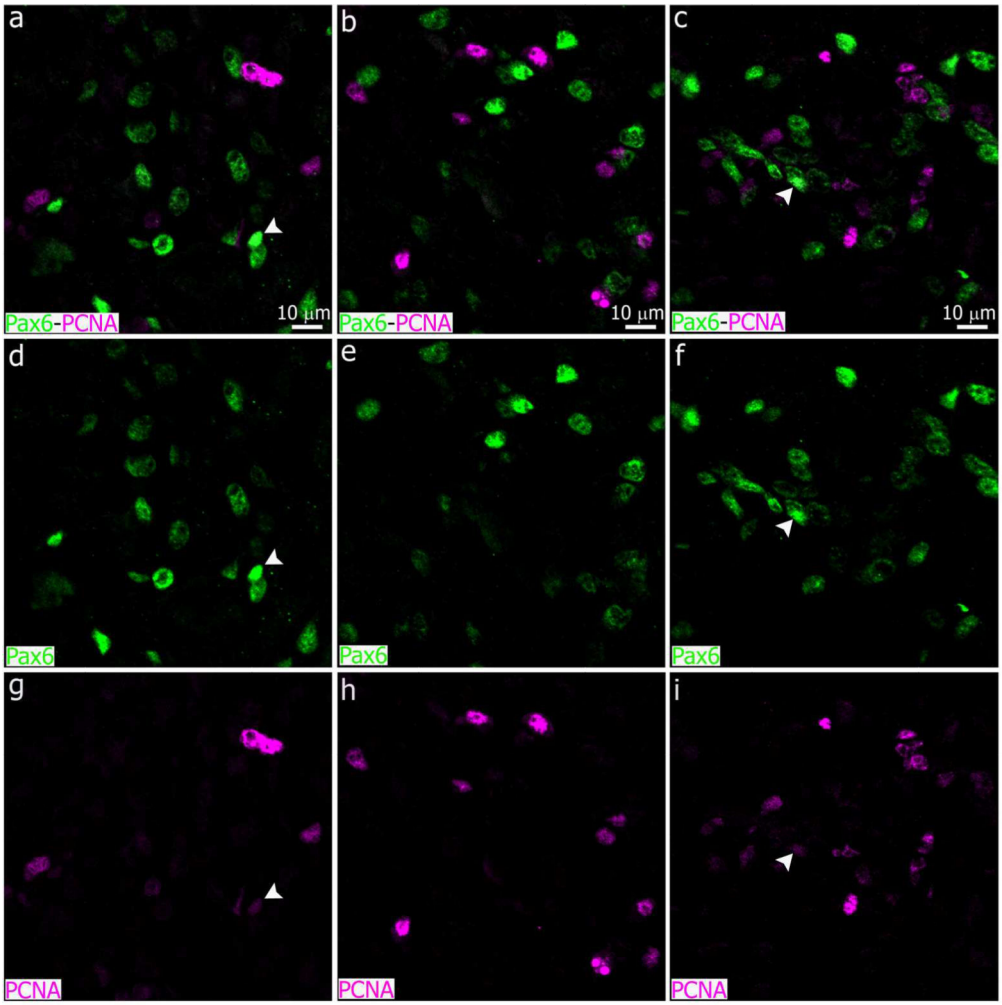

Figure 9.

The majority of Pax6^{+} cells did not express the mitotic cell marker PCNA in the pineal gland at four days after SCGd, SCGx or sham-operation. Panels show confocal images of pineal glands (PG) from control (left column, a, d, g), SCGd (center column, b, e, h) and SCGx (right column, c, f, i) rats, immunolabeled for the essential transcription factor Pax6 (green) and the proliferative marker PCNA (magenta). Pax6^{+} cells are mostly negative for PCNA (Pax6^{+}/PCNA^{-} cells). White arrowheads point Pax6^{high} cells with minimally detectable levels of the mitotic cell marker PCNA (Pax6^{high}/PCNA^{low} cells). (a-i) 3x digital zooms from 40x images; scale bar: 10 μm.

Author Manuscript Author Manuscript Author Manuscript Author Manuscript

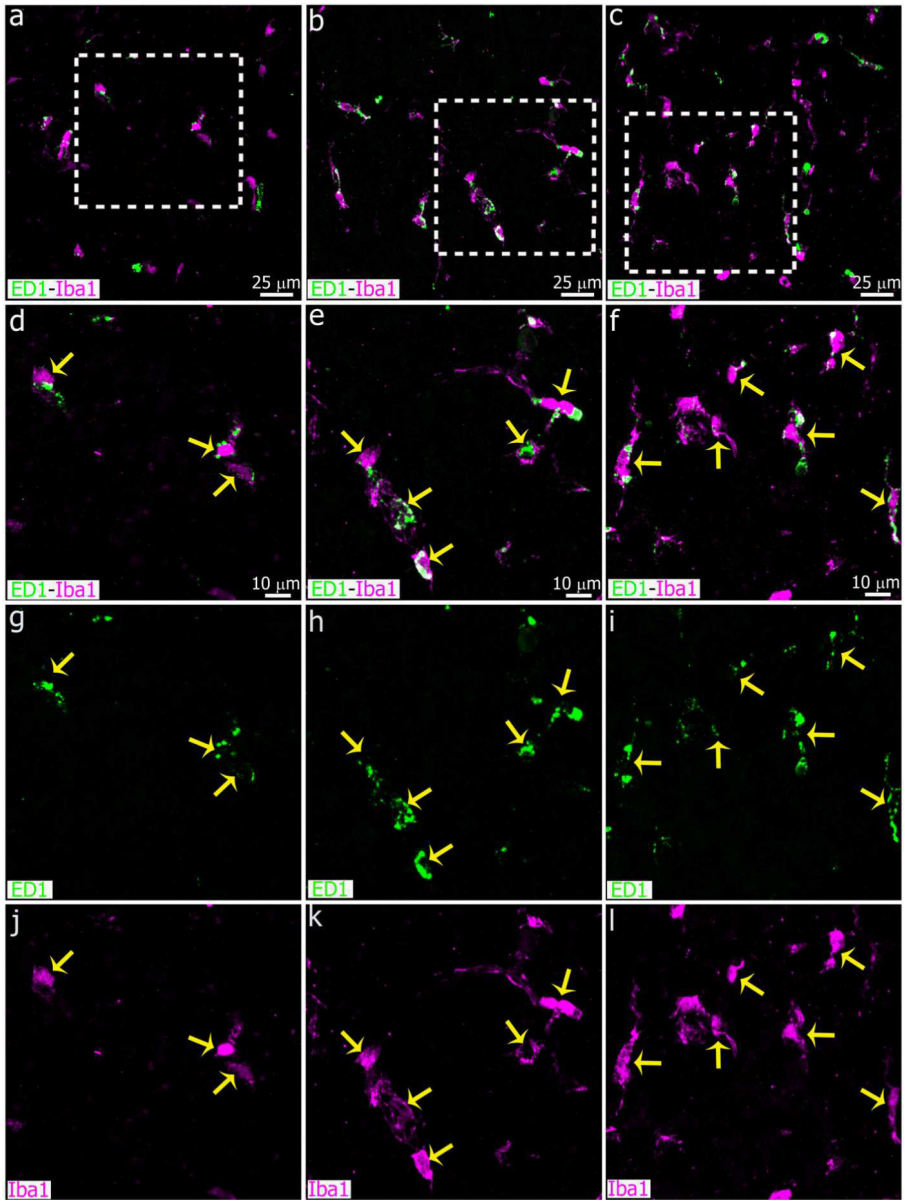

Figure 10.

The number of microglial cells that express markers associated with phagocytosis increased in the adult pineal gland four days after SCGx or SCGd. Confocal images show the proportion of Iba1^{+} microglia (magenta) that co-express the lysosomal marker ED1 (CD68, green). Although microglia in the healthy adult pineal gland (PG) normally exhibit morphological hallmarks of activation (Ibanez Rodriguez et al., 2016), the expression of ED1 was potentiated by both SCGx (right column, c, f, i, l) and SCGd (center column, b, e, h, k), compared to the sham surgery (left column, a, d, g, j). Yellow arrows indicate microglia positive for Iba1 and ED1. (a-c) 1.4x digital zooms from 40x images; scale bar: 25 μm. (d-l) 1.9x digital zooms from the insets shown in a-c; scale bar: 10 μm.

Author Manuscript
Author Manuscript
Author Manuscript
Author Manuscript

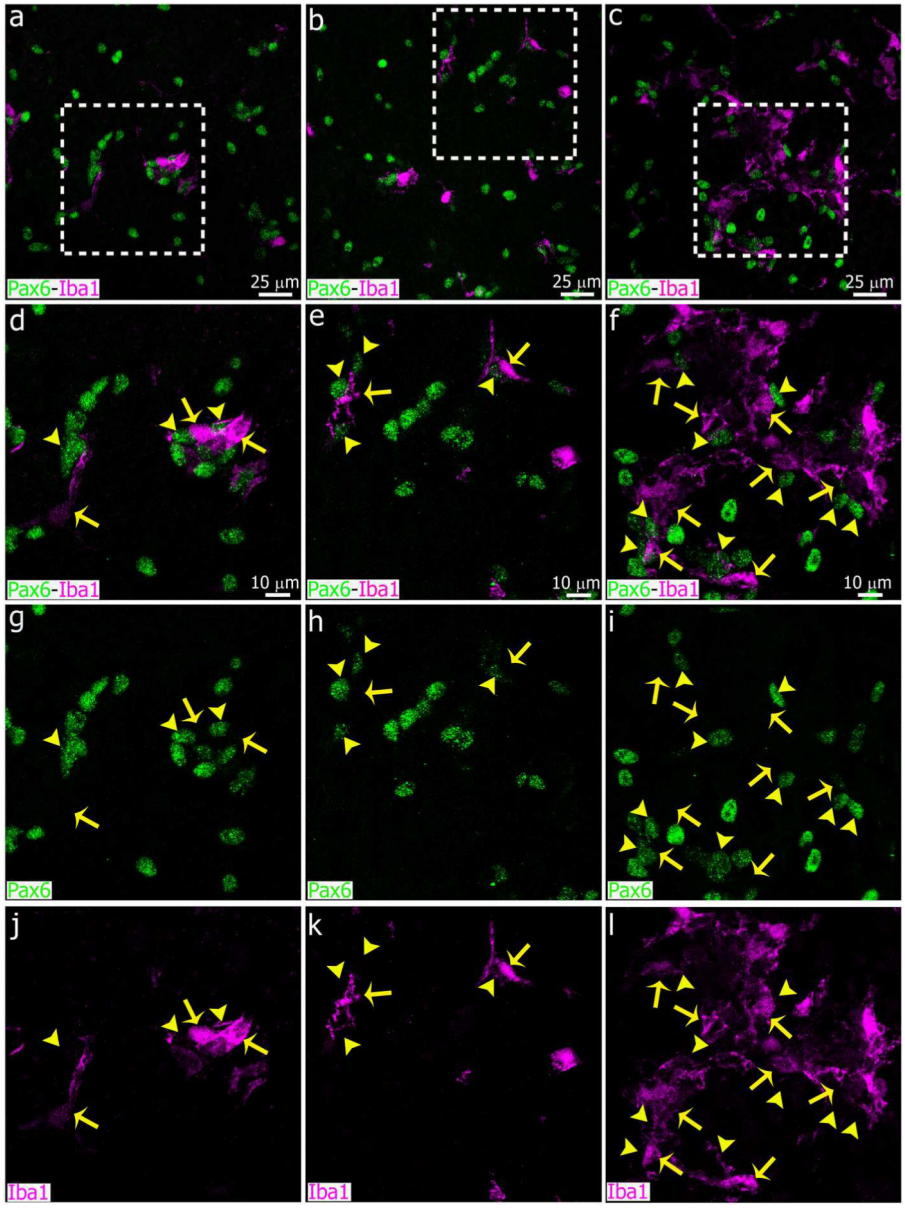

Figure 11.

An increased number of microglial cells arranged in clusters and associated with Pax6^{+} cells is observed in the pineal gland after peripheral administration of bacterial lipopolysaccharides (LPS). Panels show confocal images of the adult pineal gland (PG) after intraperitoneal (IP) injections of LPS (right column, c, f, i, l), the antibiotic doxycycline (DOX; center column, b, e, h, k), or vehicle control (left column, a, d, g, j). Close association and phagocytosis of Pax6^{+} cells (green, yellow arrowheads) by Iba1^{+} microglia (magenta, yellow arrows) were observed in the three groups. Large microglial cell clusters that encapsulated multiple Pax6^{+} cells were observed only after LPS administration. (a-c) 60x; scale bar: 25 μm. (d-l) 1.8x digital zooms from the insets shown in a-c; scale bar: 10 μm.

Author Manuscript Author Manuscript Author Manuscript Author Manuscript

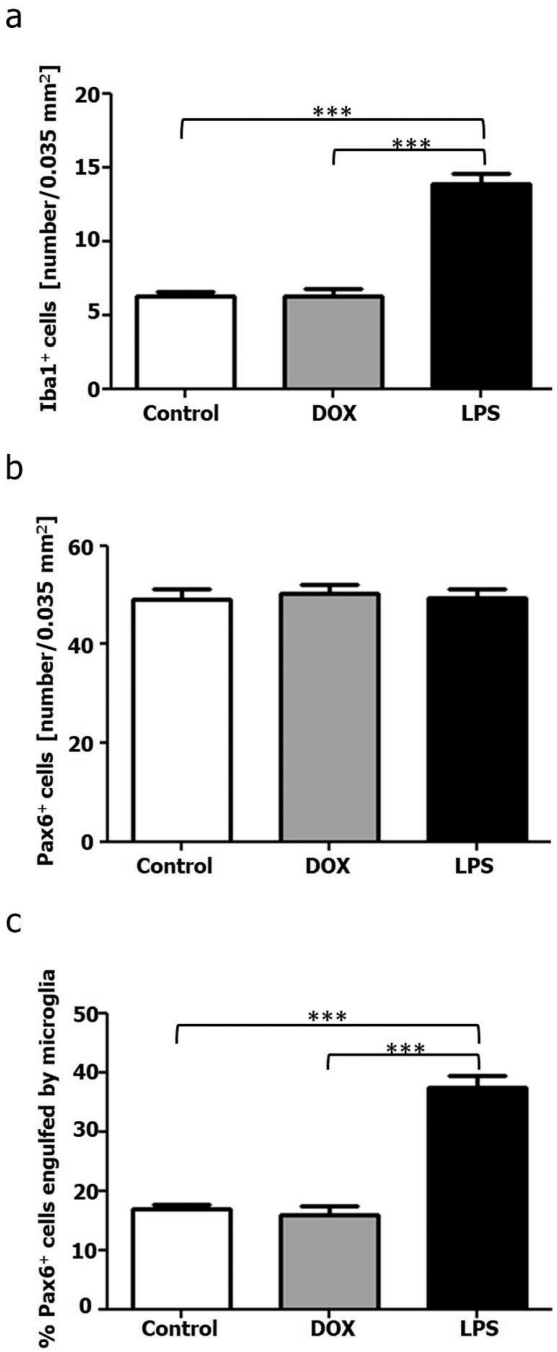

Figure 12.

The density of Iba1$^+$ microglial cells and the percentage of Pax6$^+$ cells contacted by and/or engulfed by microglia increased in the pineal gland after a peripheral challenge with bacterial lipopolysaccharides (LPS) (a and c). (b) The number of Pax6$^+$ cells in the pineal gland (PG) 24 hours after the second intraperitoneal (IP) injection of LPS was not altered. (a-c) Administration of the antibiotic doxycycline (DOX) did not affect the parameters analyzed. Data were expressed as mean ± S.E.M., in an area of 0.035 mm^2 (N=5). Statistics: one-way ANOVA followed by the Tukey post-test; ***$P < 0.001$.

Author Manuscript
Author Manuscript
Author Manuscript
Author Manuscript

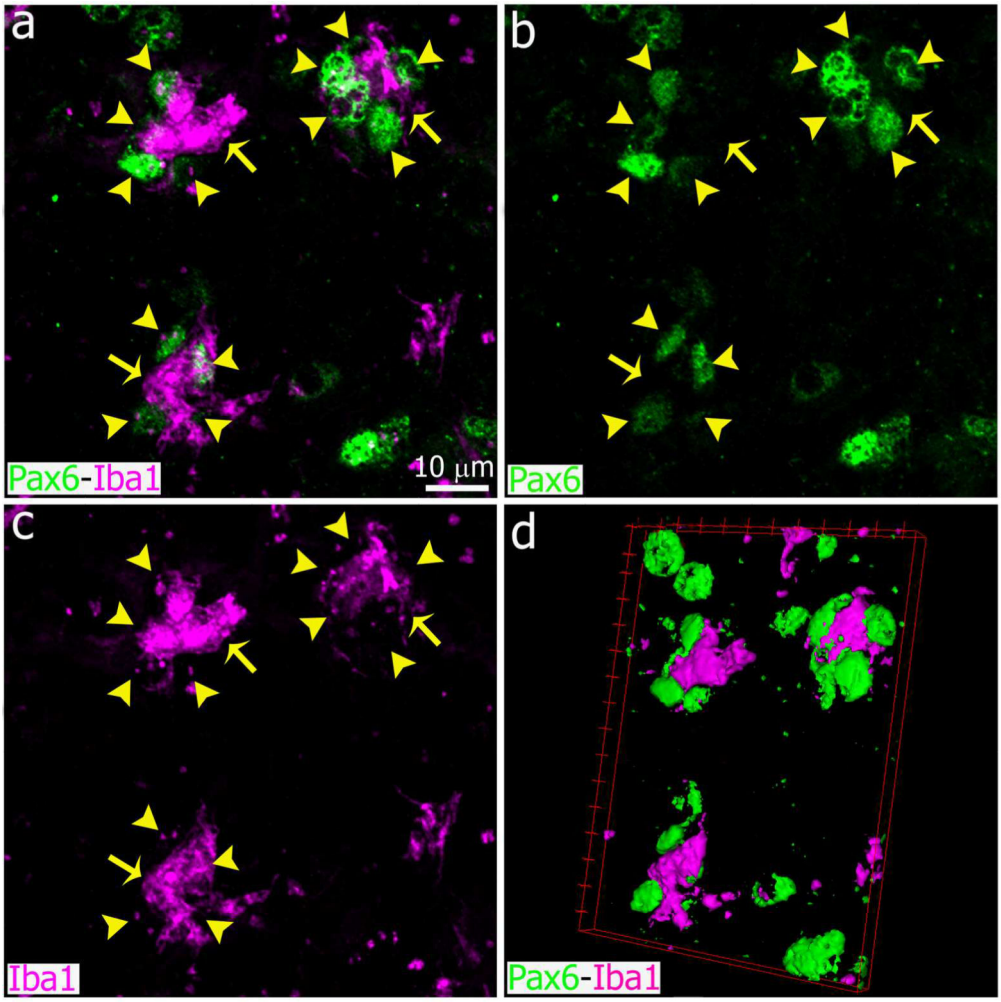

Figure 13.

Images showing representative Iba1$^+$ microglial cells and Pax6$^+$ cells in the adult pineal gland after bacterial lipopolysaccharide (LPS) administration. Each microglial cell (magenta, yellow arrows) was in contact with multiple Pax6$^+$ cells (green, yellow arrowheads), and apparently phagocytosed some of them 24 hours after the second intraperitoneal (IP) injection of LPS. (a-c) 2.8x digital zoom from a 60x image; scale bar: 10 µm. (d) 3-dimensional representation of the microglia and Pax6$^+$ cells shown in a-c.

Author Manuscript
Author Manuscript
Author Manuscript
Author Manuscript

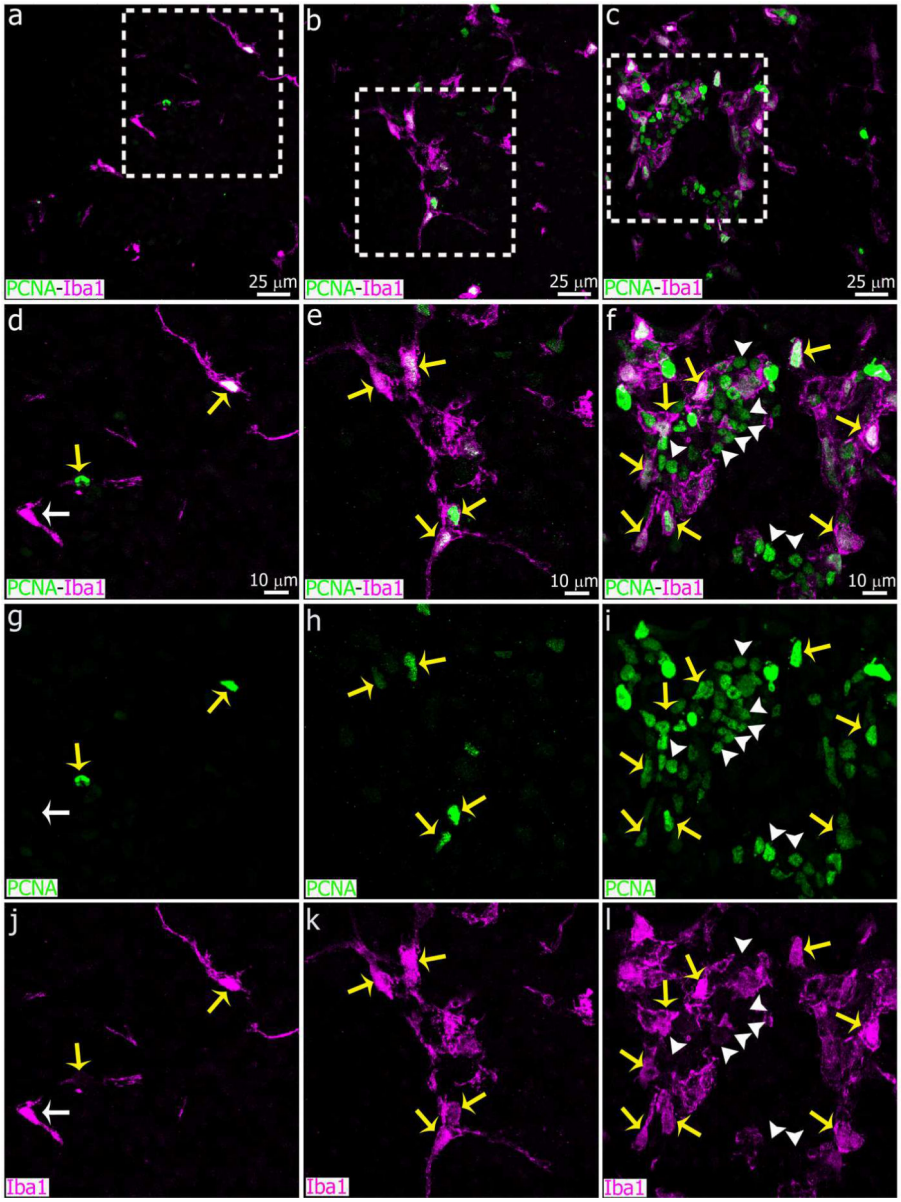

Figure 14.

Two proliferative cell populations are clearly distinguished within the microglial cell clusters induced by intraperitoneal (IP) administration of bacterial lipopolysaccharides (LPS). Sections of pineal glands (PG) immunolabeled for Iba1 (magenta) and the mitotic cell marker PCNA (green) after treatment with LPS (right column, c, f, i, l), doxycycline (DOX; center column, b, e, h, k) or vehicle (left column, a, d, g, j). In all groups, the majority of $Iba1^{+}$ microglial cells are positive for PCNA (yellow arrows). In the LPS group, a second cell population immunoreactive only for PCNA (white arrowheads) was observed within the microglial cell clusters. White arrows point an $Iba1^{+}$ microglial cell negative for PCNA in a control pineal gland. (a-c) 60x; scale bar: 25 µm. (d-l) 1.8x digital zooms from the insets shown in a-c; scale bar: 10 µm.

Author Manuscript Author Manuscript Author Manuscript Author Manuscript

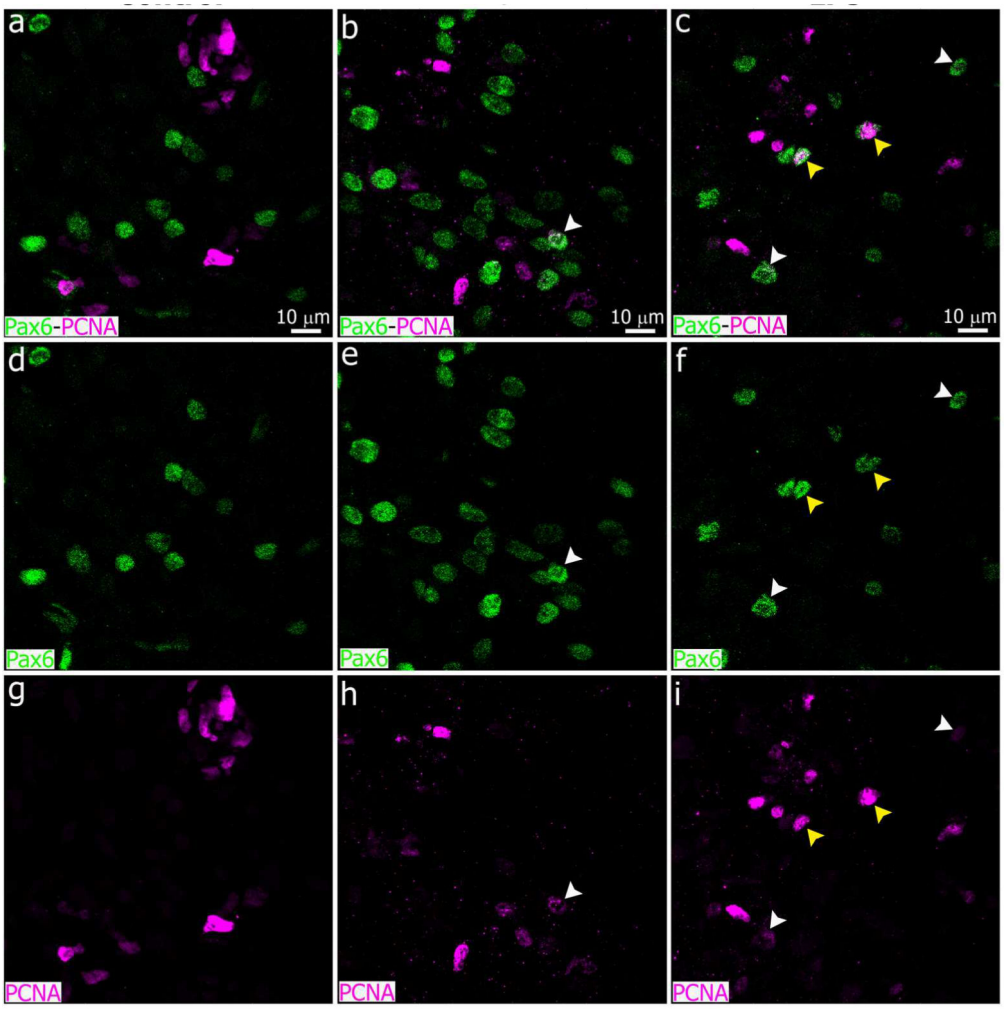

Figure 15.

Pax6^{+} cells appear to be mostly negative for the mitotic cell marker PCNA 24 hours after administration of bacterial lipopolysaccharides (LPS) or the antibiotic doxycycline (DOX). Panels show sections of pineal glands (PG) from LPS (right column, c, f, i), DOX (center column, b, e, h), or vehicle-treated (left column, a, d, g) animals, immunostained for Pax6 (green) and PCNA (magenta). The majority of the Pax6^{+} cells did not express PCNA, indicating they were not actively proliferating at ZT6. A few Pax6^{high}/PCNA^{high} cells (yellow arrowheads) were observed in the LPS-treated PGs. Pax6^{high}/PCNA^{low} cells (white arrowheads) were present in both DOX and LPS groups. (a-i) 2x digital zooms from 60x images; scale bar: 10 μm.

Author Manuscript Author Manuscript Author Manuscript Author Manuscript

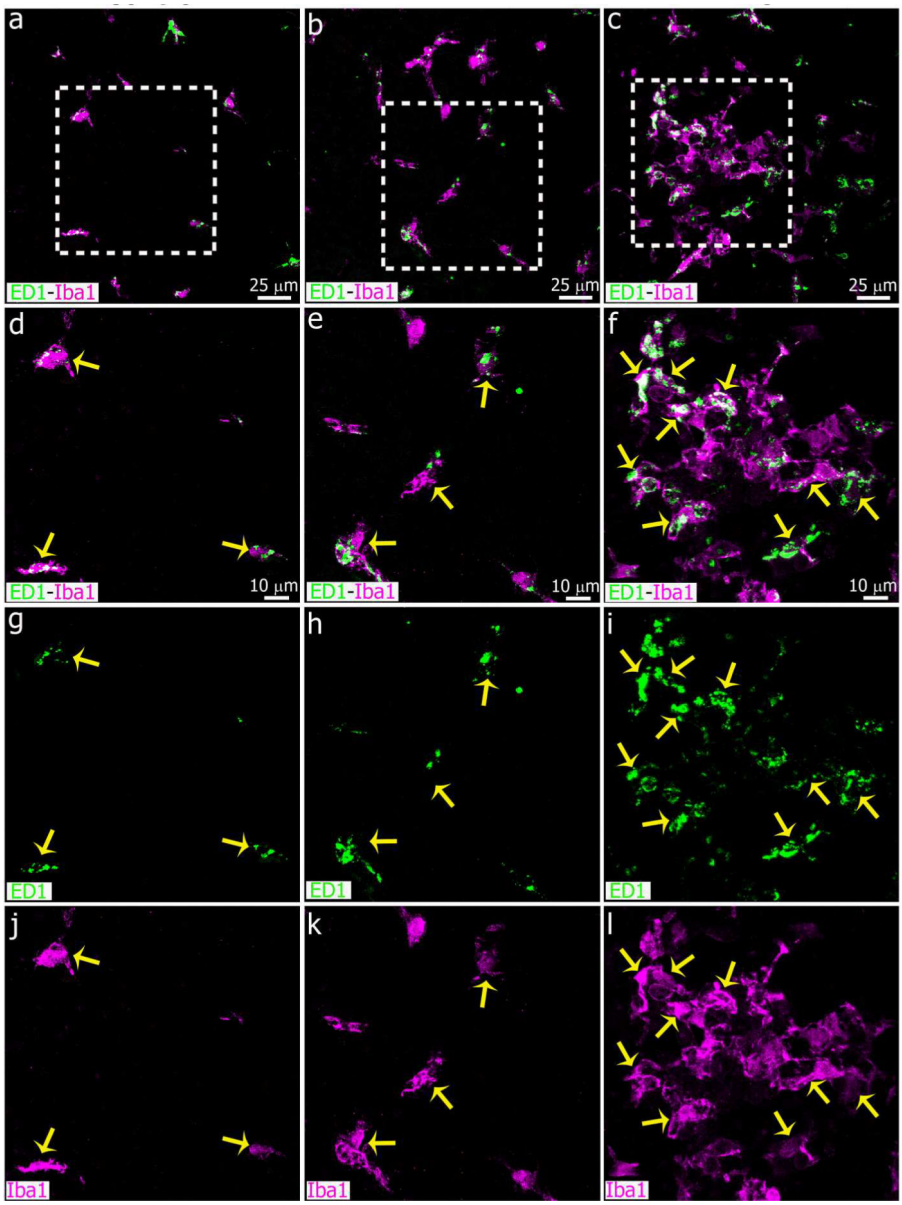

Figure 16.

Microglia are highly phagocytic after IP administration of bacterial lipopolysaccharides (LPS). Panels show images of pineal glands (PG) immunostained for Iba1 (magenta) and the lysosomal marker ED1 (CD68, green) after intraperitoneal (IP) injections of LPS (right column, c, f, i, l), doxycycline (DOX; center column, b, e, h, k) or vehicle (left column, a, d, g, j). Microglia in the cell clusters in LPS-treated pineal glands are enriched in cytoplasmic ED1-positive bodies. There were no differences in the ED1 expression pattern between control and DOX-treated PGs. Yellow arrows show microglial cells immunoreactive for both Iba1 and ED1. (a-c) 60x; scale bar: 25 µm. (d-l) 1.8x digital zooms from the insets shown in a-c; scale bar: 10 µm.

Author Manuscript Author Manuscript Author Manuscript Author Manuscript

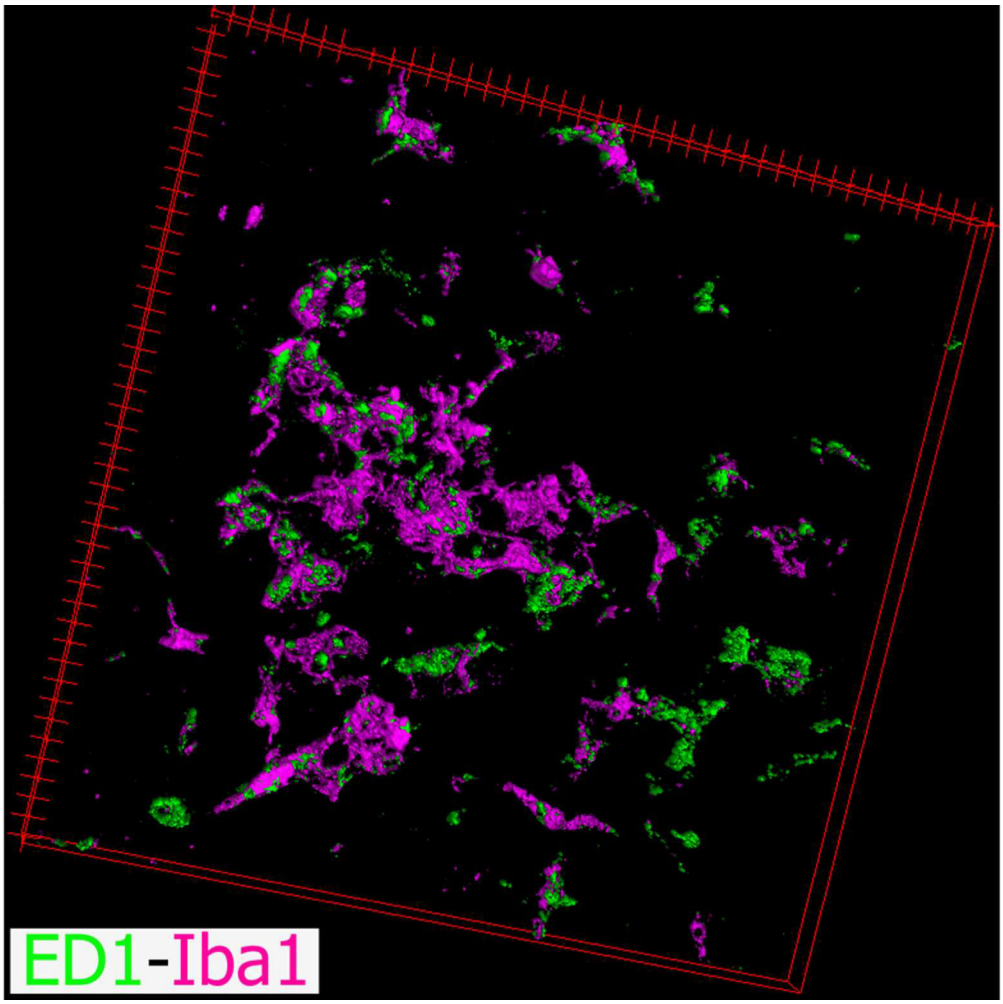

Figure 17.
Three-dimensional projection of the image shown in Figure 16c. Microglial cells (Iba1, magenta) expressing high levels of the lysosomal antigen ED1 (CD68, green) were observed in the pineal gland (PG) following intraperitoneal (IP) administration of bacterial lipopolysaccharides (LPS).

Author Manuscript Author Manuscript Author Manuscript Author Manuscript

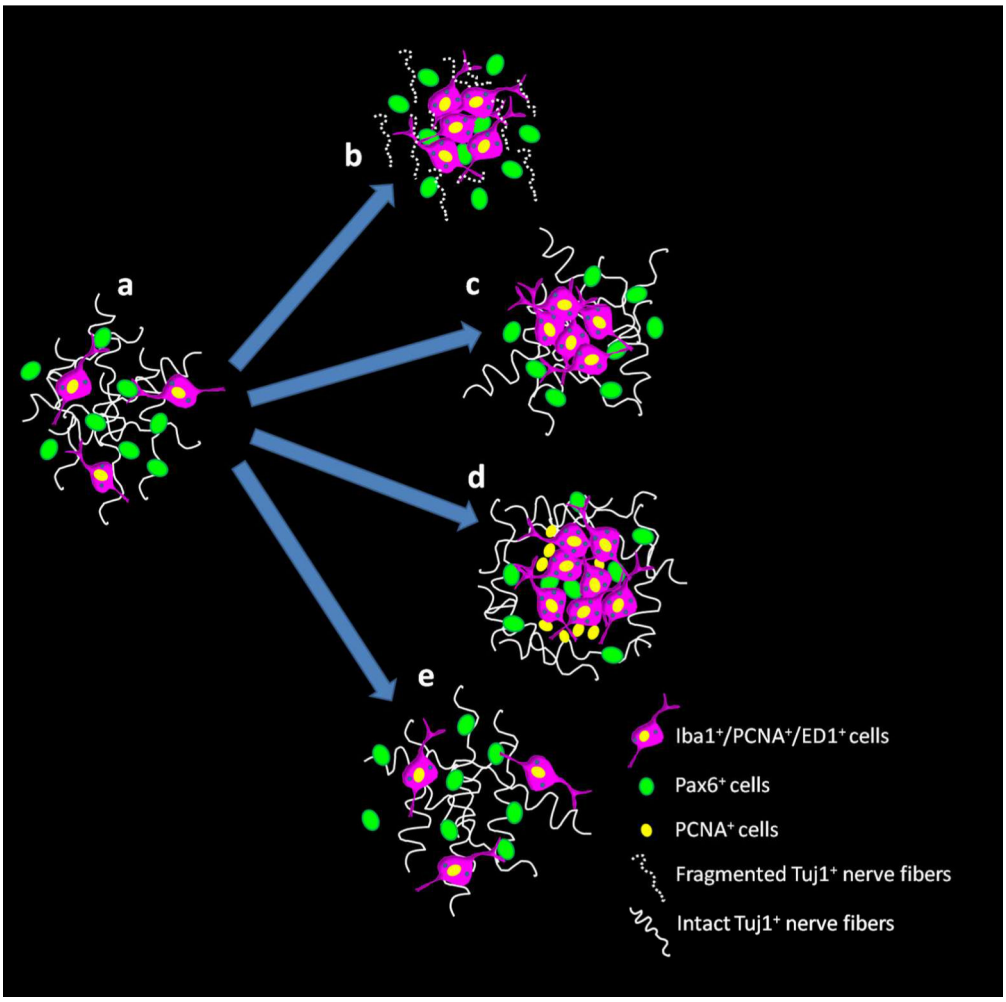

Figure 18.

Schematic model of the differential response of pineal microglia to surgical and pharmacological stimuli. (a) In the naive adult rat pineal gland (PG), microglial cells are proliferative and display hallmarks of activation and phagocytic activity ($Iba1^+/PCNA^{+/}$ $ED1^+$ cells) (Ibanez Rodriguez et al., 2016). $Pax6^+$ cells that appear to derive from $Pax6^+/$ $Vimentin^+$ neuroepithelial precursor cells in the developing pineal gland, remain in the adult gland as a quiescent cell reservoir and a preferred target for the microglial cells (Ibanez Rodriguez et al., 2016). (b) Bilateral superior cervical ganglionectomy (SCGx) induces Wallerian degeneration (WD) of the sympathetic nerve fibers that innervate the pineal gland and an increase in the density of microglial cells and $Pax6^+$ cells, and interactions between both cell types. (c) Superior cervical ganglia decentralization (SCGd) is a more subtle disruption of the sympathetic innervation to the pineal gland that increases microglial cell number without significantly altering the $Pax6^+$ cell population, or interactions between microglia and $Pax6^+$ cells. SCGd does not cause WD of the sympathetic nerve fibers. (d) Intraperitoneal (IP) administration of bacterial lipopolysaccharides (LPS) significantly increases the number of microglia in the pineal gland and induces the formation of microglial cell clusters that include at least two cell populations immunoreactive for the mitotic cell marker PCNA. LPS enhanced the association and interaction between pineal

Author Manuscript Author Manuscript Author Manuscript Author Manuscript

microglia and Pax6^{+} cells, without significantly affecting the number of Pax6^{+} cells. (e) In the rat pineal gland, doxycycline (DOX) injections did not alter the density of microglial cells or Pax6^{+} cells, and did not influence interactions between both cell types.

Author Manuscript Author Manuscript Author Manuscript Author Manuscript

Table 1.

Primary antibodies

Antibody /Clone	Host	Antigen	Source	Catalog no./RRID	Dilution
ED1	Mouse	Rat ED1 protein; also known as rat CD68.	Bio-Rad/ AbD Serotec	Cat# MCA341GA RRID: AB_566872	1:100
Iba1	Goat	Synthetic peptide corresponding to the C-terminus of human Iba1 (amino acids 135–147, TGPPAKKAISELP). This sequence is conserved in rat and mouse.	Abcam	Cat# ab5076 RRID: AB_2224402	1:200
Iba1	Rabbit	Synthetic peptide corresponding to the Iba1 C-terminal sequence (amino acids PTGPPAKKAISEL P), which is conserved among human, rat and mouse.	Wako	Cat# 019–19741 RRID: AB_839504	1:200
Pax6 (Clone AD2.38)	Mouse	Recombinant full length protein corresponding to human PAX6.	Abcam	Cat# ab78545 RRID: AB_1566562	1:100
Pax6	Rabbit	Peptide derived from the C-terminus of the mouse Pax6 protein (amino acids QVPGSEPDMSQY WPRLQ). This sequence is conserved in rat.	BioLegend /Covance	BioLegend: Cat# 901301 RRID: AB_2565003 Covance: Cat# PRB-278P RRID: AB_291612	1:200
PCNA (Clone PC10)	Mouse	Rat PCNA made in the protein A vector pR1T2T.	EMB Millipore	Cat# MAB424 RRID: AB_95106	1:100
Tuj1	Mouse	Microtubules derived from rat brain.	BioLegend /Covance	BioLegend: Cat# 801201 and 801202 RRID: AB_10063408 Covance: Cat# MMS-435P RRID: AB_2313773	1:500

Author Manuscript
Author Manuscript
Author Manuscript
Author Manuscript

Table 2.

Secondary antibodies

Antibody/Species/Host	Source/Catalog no./RRID	Dilution
Alexa Fluor 488-AffiniPure Anti-Rabbit Donkey IgG (H+L) (Min X Bov, Ck, Gt, GP, Sy Hms, Hrs, Hu, Ms, Rat, Shp Sr Prot) Antibody	Jackson Immuno Research Labs, Cat# 711–545-152, RRID: AB_2313584	1:200
Alexa Fluor 647-AffiniPure Anti-Goat Donkey IgG (H+L) (min X Ck, GP, Sy Hms, Hrs, Hu, Ms, Rb, Rat Sr Prot) Antibody	Jackson Immuno Research Labs, Cat# 705–605-147, RRID: AB_2340437	1:200
Cy3-AffiniPure Anti-Mouse Donkey IgG (H+L) (min X Bov, Ck, Gt, GP, Sy Hms, Hrs, Hu, Rb, Rat, Shp Sr Prot) Antibody	Jackson Immuno Research Labs, Cat# 715–165-151, RRID: AB_2315777	1:200

Bov: Bovine. Ck: Chicken. GP: Guinea Pig. Gt: Goat. H: Heavy Chain. Hu: Human. Hrs: Horse. L: Light Chain. Min X: Minimal Cross-Reactivity. Ms: Mouse. Rat Sr Prot: Rat Serum Proteins. Rb: rabbit. Shp Sr Prot: Sheep Serum Proteins. Sy Hms: Syrian Hamster.